Chapter 3

Characterization of RND proteins in the *Burkholderia* genus

Burkholderia species are **highly resistance to antibiotics** (Mahenthiralingam et al., 2005, Drevinek & Mahenthiralingam, 2010) especially thanks to the cooperation between the outer membrane barrier and the expression of efflux systems. In particular those belonging to RND superfamily are mainly responsible for the intrinsic drug resistance of Gram-negative bacteria (Li & Nikaido, 2004, Murakami & Yamaguchi, 2003).

RND proteins have been extensively studied in many organisms, mainly in *E. coli* and *P. aeruginosa*. Much less information are available on RND proteins in the *Burkholderia* genus. In 2010 , in our laboratory, an *in silico* analysis of RND proteins belonging to HAE-1 and HME families in 21 completely sequenced *Burkholderia* genomes allowed to determine the presence and distribution of these transporters (Perrin et al., 2010). Some of these proteins have been experimentally characterized in recent years mostly in *B. pseudomallei* and in *B. cenocepacia* species.

In *B. pseudomallei* 10 operons that may encode for RND efflux pump components were identified (Holden *et al.*, 2004, Kumar *et al.*, 2008, Perrin et al., 2010) (Figure 12). Only three of these systems have been characterized in detail, AmrAB–OprA, BpeAB–OprB and BpeEF–OprC (Schweizer, 2012).

Regarding Bcc species, RND proteins have been studied mainly in *B. cenocepacia* J2315 strain. In its genome 16 genes encoding putative RND proteins (belonging to HAE-1 and HME families) have been identified and named RND-1 to RND-16, and most of them belonging to a tri-cistronic operon embedding also genes coding for MFP and OMP proteins (Holden et al., 2009, Guglierame *et al.*, 2006, Buroni *et al.*, 2009, Perrin et al., 2010)

Five of them, that is the RND1 (BCAS0591-BCAS0593), RND2 (BCAS0764-BCAS0766), RND3 (BCAL1674-BCAL1676), RND-4 (BCAL2820-BCAL2822) and *ceo* (RND-10, BCAM2549-BCAM2551) operons, all belonging to HAE-1 family, have been experimentally characterized (Burns *et al.*, 1989, Burns *et al.*, 1996, Nair *et al.*,

2004, Nair *et al.*, 2005, Guglierame et al., 2006, Buroni et al., 2009). Also HpnN transporters were identified and characterized in *B. cenocepacia* and in *B. multivorans* where they are involved in antibiotics resistance (Schmerk et al., 2011, Malott *et al.*, 2012).

The characterization of RND proteins in the *Burkholderia* genus performed during this PhD, involved the use of two different approaches, an *in silico* one and a wet-lab one. In addition some natural extract were tested both on the 18 Bcc type strains and on some RND operons deletion mutants, in order to find new antimicrobial compounds or efflux pumps inhibitors (Figure 14).

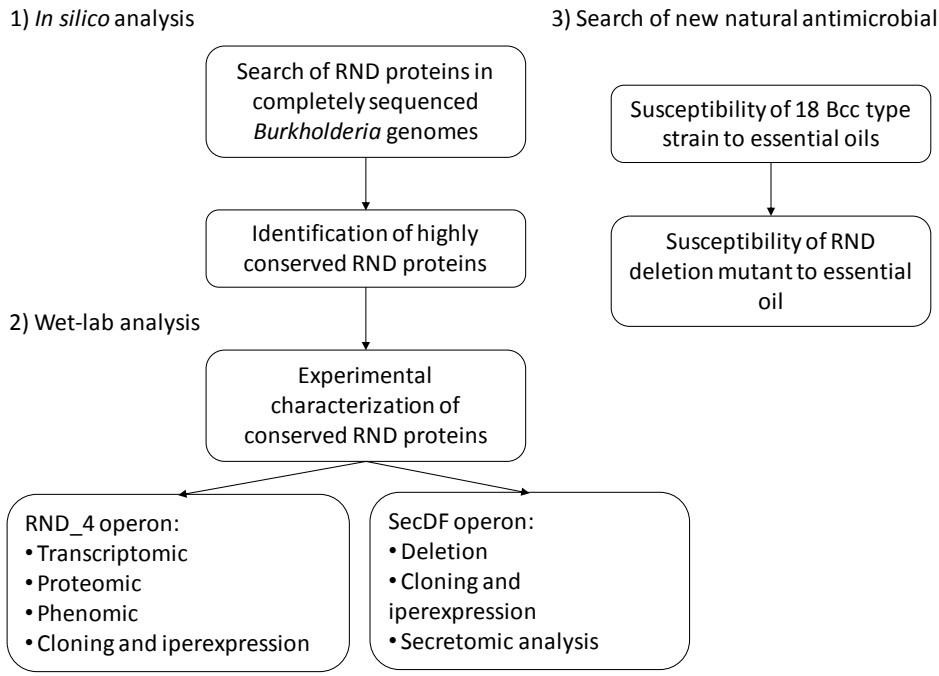

Figure 14: Experimental strategy of the characterization of RND proteins in the *Burkholderia* genus

Regarding the *in silico* approach, the analysis of all the eight RND families in 26 completely sequenced *Burkholderia* genomes was performed (Perrin *et al.*, 2013).

A total of 417 putative RND sequences were identified and analyzed at different levels, using different bioinformatics tools that allowed the assignment of a putative function to the majority of them. In particular, 232 sequences have been assigned to the HAE-1 family, involved in antibiotic resistance, 37 sequences were affiliated to the HME family (heavy-metal-efflux), and 39 sequences fell in a cluster probably representing a new and not yet characterized RND family (UF).

One copy of highly conserved *secD* and *secF* as well as the putative hopanoid transporter HpnN was detected in all the 26 *Burkholderia* genomes. The *hnpN* gene was always associated with the SHC gene that is essential for hopanoid biosynthesis (Schmerk et al., 2011). A group of putative APPE proteins was identified and only 24 sequences (divided into four different clusters, 27, 30, 31 and 32) were not assigned to any RND family. Indeed, although they retain the characteristic structure of the RND proteins, it has not been possible to obtain any information regarding their function.

A *core* of RND proteins conserved in all genomes analyzed was identified: at least one copy of the genes belonging to the HAE-1 and SecDF families and to HpnN transporters is present in all the genomes analyzed.

On the basis of these analysis and of the data obtained in the previous work (Perrin et al., 2010), some highly conserved RND proteins in the *Burkholderia* species were further characterized from an experimental viewpoint . Indeed, their high degree of conservation suggests that they could play a key role in these microorganisms. In particular two operons were chosen to a further characterization in the model systems *B.cenocepacia* J2315: the **RND-4 operon**, since it is one of the most conserved of those belonging to HAE-1 family (Perrin et al., 2010) and seems to be involved multi-drug resistance (Buroni et al., 2009), and the SecDF operon, for its high conservation (Perrin et al., 2013) and because it has been demonstrated in other bacteria that these proteins complex is involved in antibiotics resistance and

secretion of virulence factors (Quiblier *et al.*, 2011, Quiblier *et al.*, 2013, Burg-Golani *et al.*, 2013).

A *B. cenocepacia* J2315 mutant strain impaired in RND-4 efflux system, referred to asD4 (ΔBCAL2820-BCAL2822), was obtained in the laboratory of Prof. Giovanna Riccardi at the University of Pavia (Buroni et al., 2009) and was characterized from a transcriptomic, phenomic and proteomic viewpoint (Bazzini *et al.*, 2011, Gamberi *et al.*, 2013).

Phenomic and transcriptomic analyses were performed on D4 mutant and on two others RND mutants. The first was a *B cenocepacia* J2315 mutant strain impaired in RND-9 operon, called D9 (ΔBCAM1945-BCAM1948, where also the associated MerR transcriptional regulator, encoded by BCAM1948 gene, was deleted), which was chosen because BCAM1947 gene was found to be over -expressed in the *sputum* of CF patients (Drevinek *et al.*, 2008). The second strain is a double mutant impaired in both RND4 e RND9 operons, called D4-D9 (Bazzini et al., 2011).

For the phenomic analysis the Phenotype MicroArray (PM) procedure was used (Bochner *et al.*, 2001, Bochner *et al.*, 2008). PM is a technology allowing to quantitatively measure thousands of cellular phenotypes all at once. Ten different panels (PM11-PM20) that enable chemical sensitivity test for bacteria were analyzed. Data obtained revealed that RND-4 is involved in the extrusion of a wide variety of toxic compounds, in agreement with antimicrobial susceptibilities of the mutant previous determined (Buroni et al., 2009), and similar results were obtained also for the double mutant D4-D9. Conversely, D9 strain showed a phenotype very similar to the wild type (w.t.) strain J2315. This could be due to the fact that in D9 mutant the RND-9 function could be replaced by other efflux systems, alternatively, the RND-9 might be involved in the efflux of molecules under different physiological conditions than those utilized in this work.

Also microarray analysis confirmed a similarity between D4 and D4-D9 mutants. Indeed, these two strains exhibit a similar expression profile; in particular motility

and chemotaxis-related genes appear to be up-regulated in both , while the same genes are down-regulated or not differentially expressed in D9 mutant. Data from microarray were in agreement with those coming from the motility assays, in which the D4 and the D4-D9 double mutant showed enhanced swimming motility in respect to the wt, in contrast with mutant D9 where this phenomenon is reduced. Moreover, D4 has 12 more up-regulated genes involved in motility than D4-D9; this might explain way this mutant is more mobile than the double mutant. It seems that D9 mutation is able to partially suppress the effects of the D4 mutation, at least for what concerns swimming.

Regarding chemotaxis, despite the differences observed in the microarray analysis, the three mutants showed the same phenotype under our experimental conditions, but it is possible that differences might be appreciated by the use of specific attractant or repellent molecules.

All the three mutants showed also an enhanced biofilm production, despite no genes obviously involved in biofilm formation were identified among those having the same expression pattern in the three microarray experiments.

Overall, data obtained in this work strongly suggest that the biological role of RND proteins might not be restricted to the sole transport of toxic compounds.

These results are in agreement with data obtained from proteomic analysis performed on D4 mutant that suggest that the effect of this deletion is not "narrowed" to extrusion of toxic compounds (Gamberi et al., 2013). In particular, the intracellular proteome of the deletion mutant was compared with that of the wt *B. cenocepacia* J2315 using two-dimensional electrophoresis and 49 of the 70 differentially expressed proteins were identified by mass spectrometry. The amount of some proteins involved in amino acid transport and metabolism, translation and nucleotide synthesis are lower in D4 mutant suggesting a decreased protein and DNA synthesis in this strain. Moreover, the level of four proteins

involved in peptidoglycan biosynthesis are also down-regulated and these data may reflect an alteration in plasma membrane permeability and cell wall composition.

Among the up-regulated proteins in mutant D4, proteins involved in post-translational modification, protein turnover or chaperones were identified. The higher content of these proteins is consistent with the presence of environmental stresses in the mutant strain. All the changes observed could be the consequence of the stress condition connected to the loss of the RND-4 operon or they could be linked to the physiological role of these proteins.

To further characterize RND-4 operon, its cloning is in progress, with two main purpose. The first is the complementation of deletion in mutant D4 to verify that the observed phenotypes are really due to the deletion of these operon. The second is to evaluate the effect of RND-4 operon iper-expression, since for example it has been demonstrated that the over-expression of AcrB can be toxic for *E.coli* (Ma et al., 1993). In addition to this, we want also verify if other RND operons, under stress conditions, can activate and compensate for the lack of RND-4. To do this also the cloning of RND-2 operon is in progress. The latter operon was chosen because it is present only in few Bcc species and its genes have a high degree of sequence similarity with RND-4 operon (Perrin et al., 2010).

However, *Burkholderia* species are not readily tractable genetically, and only very few tools and limited numbers of selection markers are available for their genetic manipulation (Flannagan *et al.*, 2008). In addition to this the large size of RND operons make them even more difficult to clone. Therefore, it was necessary to develop a two-step/two fragment strategy for operon cloning, by cloning separately the two halves of the operon that will be re-joined in the final expression vector. At the present time, we were able to clone the two halves of RND-2 and RND-4 operons in the pGEM-T Easy cloning vector, but the cloning of the two fragments in the final expression vector for *Burkholderia*, pSCrhaB2 (Cardona & Valvano, 2005), is still in progress.

Regarding the SecDF-YajC operon, the presence and conservation of these three genes in 156 *Burkholderia* genomes (both complete and draft) was determined, revealing an high degree of conservation.

Then a deletion mutant impaired in this operon was obtained and also its cloning is in progress. Once obtained the mutants strains, various type of analysis will be carried out: the susceptibility to different classes of antibiotics, the virulence in a *C. elegans* host model and a secretome analysis to identify virulence factors that could be secreted by this operon.

Regarding the susceptibility of Bcc strains to some essential oils (EOs) they consist of a complex blend of volatile and fragrant substances typically synthesized by all plant organs as secondary metabolites and extracted by water or steam distillation, solvent extraction, expression under pressure, supercritical fluid and subcritical water extractions (Bassole & Juliani, 2012). EOs possess antibacterial, antifungal and antiviral properties and have been screened worldwide as potential sources of novel antimicrobial compounds (Solorzano-Santos & Miranda-Novales, 2012) The antimicrobial properties of EOs have been reported in several studies and the mechanisms by which they can inhibit microorganisms involve different modes of action, and in part may be due to their hydrophobicity. It is likely that it will be more difficult for bacteria to develop resistance to the multi-component EOs than to common antibiotics that are often composed of only a single molecular entity (Solorzano-Santos & Miranda-Novales, 2012). Moreover, over the past few years, several natural compounds acting as efflux pump inhibitors have been investigated (Webber & Piddock, 2003, Jodoin *et al.*, 2002, Lorenzi *et al.*, 2009, Stavri *et al.*, 2007, Stermitz *et al.*, 2000). Some of them able to restore the activity of usual antibiotics on resistant clinical bacteria isolated during therapeutic treatment (Fadli *et al.*, 2011).

In our work six different essential oils (*Eugenia caryophyllata*, *Origanum vulgare*, *Rosmarinus officinalis, Lavandula officinalis, Melaleuca alternifolia* and *Thymus*

vulgaris) were tested *vs* the 18 type strains of the known Bcc species (Maida *et al.* manuscript in preparation)

The composition of the six EOs was quite different but, in spite of this, all of them exhibited an inhibitory activity *vs* all the 18 Bcc strains, suggesting that one compound, or more likely more than one compounds (see below) present in each essential oil possessed might interfere with the Bcc cell growth. However, the six essential oils showed a different inhibitory activity and, according to Ponce et al (2003) (Ponce *et al.*, 2003) they might be split into two different clusters; the first one includes *Thymus vulgaris, Origanum vulgare* and *Eugenia caryophyllata*, whereas the other one embeds *Rosmarinus officinalis, Maleuca alternifolia* and *Lavandula officinalis.* Indeed, Bcc strains were extremely sensitive to the EOs belonging to the first group and just sensitive to the other three.

However, all of them are able to inhibit the growth of Bcc strains; particularly interesting and intriguing is the finding that the inhibitory halos produced by most of EOs are (much more) larger than that produced by ciprofloxacin, one of the antibiotics used in CF infections therapy.

The preliminary data reported in this work are particularly encouraging, since they demonstrate that the use of Essential Oils might represent an alternative way to fight Bcc growth.

To further investigate the mechanisms of EOs activity against Bcc species, the same 6 essential oils were tested *vs* 6 RND operons deletion mutants, a double and a triple mutants. Preliminary results obtained, showed that some of these operons are involved in the transport of some of the sub-components of the essential oils used. The characterization of other RND operons deletion mutants and the evaluation of the ability of these EOs to inhibit the activity of some of these efflux pumps is still in progress.

Bibliography

Bassole, I. H. & H. R. Juliani, (2012) Essential oils in combination and their antimicrobial properties. *Molecules* **17**: 3989-4006.

Bazzini, S., C. Udine, A. Sass, M. R. Pasca, F. Longo, G. Emiliani, M. Fondi, E. Perrin, F. Decorosi, C. Viti, L. Giovannetti, L. Leoni, R. Fani, G. Riccardi, E. Mahenthiralingam & S. Buroni, (2011) Deciphering the role of RND efflux transporters in *Burkholderia cenocepacia*. *PLoS One* **6**: e18902.

Bochner, B. R., P. Gadzinski & E. Panomitros, (2001) Phenotype microarrays for high-throughput phenotypic testing and assay of gene function. *Genome Res* **11**: 1246-1255.

Bochner, B. R., L. Giovannetti & C. Viti, (2008) Important discoveries from analysing bacterial phenotypes. *Mol Microbiol* **70**: 274-280.

Burg-Golani, T., Y. Pozniak, L. Rabinovich, N. Sigal, R. Nir Paz & A. A. Herskovits, (2013) Membrane Chaperone SecDF Plays a Role in the Secretion of *Listeria monocytogenes* Major Virulence Factors. *J Bacteriol* **195**: 5262-5272.

Burns, J. L., L. A. Hedin & D. M. Lien, (1989) Chloramphenicol resistance in *Pseudomonas cepacia* because of decreased permeability. *Antimicrob Agents Chemother* **33**: 136-141.

Burns, J. L., C. D. Wadsworth, J. J. Barry & C. P. Goodall, (1996) Nucleotide sequence analysis of a gene from *Burkholderia* (*Pseudomonas*) *cepacia* encoding an outer membrane lipoprotein involved in multiple antibiotic resistance. *Antimicrob Agents Chemother* **40**: 307-313.

Buroni, S., M. R. Pasca, R. S. Flannagan, S. Bazzini, A. Milano, I. Bertani, V. Venturi, M. A. Valvano & G. Riccardi, (2009) Assessment of three Resistance-Nodulation-Cell Division drug efflux transporters of *Burkholderia cenocepacia* in intrinsic antibiotic resistance. *BMC Microbiol* **9**: 200.

Cardona, S. T. & M. A. Valvano, (2005) An expression vector containing a rhamnose-inducible promoter provides tightly regulated gene expression in *Burkholderia cenocepacia*. *Plasmid* **54**: 219-228.

Drevinek, P., M. T. Holden, Z. Ge, A. M. Jones, I. Ketchell, R. T. Gill & E. Mahenthiralingam, (2008) Gene expression changes linked to antimicrobial resistance, oxidative stress, iron depletion and retained motility are observed when *Burkholderia cenocepacia* grows in cystic fibrosis sputum. *BMC Infect Dis* **8**: 121.

Drevinek, P. & E. Mahenthiralingam, (2010) *Burkholderia cenocepacia* in cystic fibrosis: epidemiology and molecular mechanisms of virulence. *Clin Microbiol Infect* **16**: 821-830.

Fadli, M., J. Chevalier, A. Saad, N. E. Mezrioui, L. Hassani & J. M. Pages, (2011) Essential oils from Moroccan plants as potential chemosensitisers restoring antibiotic activity in resistant Gram-negative bacteria. *Int J Antimicrob Agents* **38**: 325-330.

Flannagan, R. S., T. Linn & M. A. Valvano, (2008) A system for the construction of targeted unmarked gene deletions in the genus *Burkholderia*. *Environ Microbiol* **10**: 1652-1660.

Gamberi, T., Rocchiccioli S., Papaleo M. C., Magherini F., Citti L. , Buroni S., Bazzini S., Udine C., Perrin E., Modesti A. & F. R., (2013) RND-4 efflux transporter gene deletion in *Burkholderia cenocepacia* J2315: a proteomic analysis. *Journal of Proteome Science and Computational Biology 2013* **2:1 http://dx.doi.org/10.7243/2050-2273-2-1**

Guglierame, P., M. R. Pasca, E. De Rossi, S. Buroni, P. Arrigo, G. Manina & G. Riccardi, (2006) Efflux pump genes of the resistance-nodulation-division family in *Burkholderia cenocepacia* genome. *BMC Microbiol* **6**: 66.

Holden, M. T., H. M. Seth-Smith, L. C. Crossman, M. Sebaihia, S. D. Bentley, A. M. Cerdeno-Tarraga, N. R. Thomson, N. Bason, M. A. Quail, S. Sharp, I. Cherevach, C. Churcher, I. Goodhead, H. Hauser, N. Holroyd, K. Mungall, P. Scott, D. Walker, B. White, H. Rose, P. Iversen, D. Mil-Homens, E. P. Rocha, A. M. Fialho, A. Baldwin, C. Dowson, B. G. Barrell, J. R. Govan, P. Vandamme, C. A. Hart, E. Mahenthiralingam & J. Parkhill, (2009) The genome of *Burkholderia cenocepacia* J2315, an epidemic pathogen of cystic fibrosis patients. *J Bacteriol* **191**: 261-277.

Holden, M. T., R. W. Titball, S. J. Peacock, A. M. Cerdeno-Tarraga, T. Atkins, L. C. Crossman, T. Pitt, C. Churcher, K. Mungall, S. D. Bentley, M. Sebaihia, N. R. Thomson, N. Bason, I. R. Beacham, K. Brooks, K. A. Brown, N. F. Brown, G. L. Challis, I. Cherevach, T. Chillingworth, A. Cronin, B. Crossett, P. Davis, D. DeShazer, T. Feltwell, A. Fraser, Z. Hance, H. Hauser, S. Holroyd, K. Jagels, K. E. Keith, M. Maddison, S. Moule, C. Price, M. A. Quail, E. Rabbinowitsch, K. Rutherford, M. Sanders, M. Simmonds, S. Songsivilai, K. Stevens, S. Tumapa, M. Vesaratchavest, S. Whitehead, C. Yeats, B. G. Barrell, P. C. Oyston & J. Parkhill, (2004) Genomic plasticity of the causative agent of melioidosis, *Burkholderia pseudomallei*. *Proc Natl Acad Sci U S A* **101**: 14240-14245.

Jodoin, J., M. Demeule & R. Beliveau, (2002) Inhibition of the multidrug resistance P-glycoprotein activity by green tea polyphenols. *Biochim Biophys Acta* **1542**: 149-159.

Kumar, A., M. Mayo, L. A. Trunck, A. C. Cheng, B. J. Currie & H. P. Schweizer, (2008) Expression of resistance-nodulation-cell-division efflux pumps in commonly used *Burkholderia pseudomallei* strains and clinical isolates from northern Australia. *Trans R Soc Trop Med Hyg* **102 Suppl 1**: S145-151.

Li, X. Z. & H. Nikaido, (2004) Efflux-mediated drug resistance in bacteria. *Drugs* **64**: 159-204.

Lorenzi, V., A. Muselli, A. F. Bernardini, L. Berti, J. M. Pages, L. Amaral & J. M. Bolla, (2009) Geraniol restores antibiotic activities against multidrug-resistant

isolates from gram-negative species. *Antimicrob Agents Chemother* **53**: 2209-2211.

Ma, D., D. N. Cook, M. Alberti, N. G. Pon, H. Nikaido & J. E. Hearst, (1993) Molecular cloning and characterization of acrA and acrE genes of *Escherichia coli*. *J Bacteriol* **175**: 6299-6313.

Mahenthiralingam, E., T. A. Urban & J. B. Goldberg, (2005) The multifarious, multireplicon *Burkholderia cepacia* complex. *Nat Rev Microbiol* **3**: 144-156.

Malott, R. J., B. R. Steen-Kinnaird, T. D. Lee & D. P. Speert, (2012) Identification of hopanoid biosynthesis genes involved in polymyxin resistance in *Burkholderia multivorans*. *Antimicrob Agents Chemother* **56**: 464-471.

Murakami, S. & A. Yamaguchi, (2003) Multidrug-exporting secondary transporters. *Curr Opin Struct Biol* **13**: 443-452.

Nair, B. M., K. J. Cheung, Jr., A. Griffith & J. L. Burns, (2004) Salicylate induces an antibiotic efflux pump in *Burkholderia cepacia* complex genomovar III (*B. cenocepacia*). *J Clin Invest* **113**: 464-473.

Nair, B. M., L. A. Joachimiak, S. Chattopadhyay, I. Montano & J. L. Burns, (2005) Conservation of a novel protein associated with an antibiotic efflux operon in *Burkholderia cenocepacia*. *FEMS Microbiol Lett* **245**: 337-344.

Perrin, E., M. Fondi, M. C. Papaleo, I. Maida, S. Buroni, M. R. Pasca, G. Riccardi & R. Fani, (2010) Exploring the HME and HAE1 efflux systems in the genus *Burkholderia*. *BMC Evol Biol* **10**: 164.

Perrin, E., M. Fondi, M. C. Papaleo, I. Maida, G. Emiliani, S. Buroni, M. R. Pasca, G. Riccardi & R. Fani, (2013) A census of RND superfamily proteins in the *Burkholderia* genus. *Future Microbiol* **8**: 923-937.

Ponce, A. G., R. Fritz, C. del Valle & S. I. Rourac, (2003) Antimicrobial activity of essential oils on the native microflora of organic Swiss chard. *LWT - Food Science and Technology* **36**: 679-684.

Quiblier, C., K. Seidl, B. Roschitzki, A. S. Zinkernagel, B. Berger-Bachi & M. M. Senn, (2013) Secretome analysis defines the major role of SecDF in Staphylococcus aureus virulence. *PLoS One* **8**: e63513.

Quiblier, C., A. S. Zinkernagel, R. A. Schuepbach, B. Berger-Bachi & M. M. Senn, (2011) Contribution of SecDF to Staphylococcus aureus resistance and expression of virulence factors. *BMC Microbiol* **11**: 72.

Schmerk, C. L., M. A. Bernards & M. A. Valvano, (2011) Hopanoid production is required for low-pH tolerance, antimicrobial resistance, and motility in *Burkholderia* cenocepacia. *J Bacteriol* **193**: 6712-6723.

Schweizer, H. P., (2012) Mechanisms of antibiotic resistance in *Burkholderia pseudomallei*: implications for treatment of melioidosis. *Future Microbiol* **7**: 1389-1399.

Solorzano-Santos, F. & M. G. Miranda-Novales, (2012) Essential oils from aromatic herbs as antimicrobial agents. *Curr Opin Biotechnol* **23**: 136-141.

Stavri, M., L. J. Piddock & S. Gibbons, (2007) Bacterial efflux pump inhibitors from natural sources. *J Antimicrob Chemother* **59**: 1247-1260.

Stermitz, F. R., P. Lorenz, J. N. Tawara, L. A. Zenewicz & K. Lewis, (2000) Synergy in a medicinal plant: antimicrobial action of berberine potentiated by 5'-methoxyhydnocarpin, a multidrug pump inhibitor. *Proc Natl Acad Sci U S A* **97**: 1433-1437.

Webber, M. A. & L. J. Piddock, (2003) The importance of efflux pumps in bacterial antibiotic resistance. *J Antimicrob Chemother* **51**: 9-11.

Research Article
Future Microbiology

A census of RND superfamily proteins in the *Burkholderia* genus

Elena Perrin[‡1], Marco Fondi[‡1,2], Maria Cristiana Papaleo[1], Isabel Maida[1], Giovanni Emiliani[3], Silvia Buroni[4], Maria Rosalia Pasca[4], Giovanna Riccardi[4] & Renato Fani[*1]

[1]Laboratory of Molecular & Microbial Evolution, Department of Biology, University of Florence, Via Madonna del Piano 6, 50019 Sesto Fiorentino (FI), Italy
[2]Computer Laboratory, University of Cambridge, Cambridge, UK
[3]Trees & Timber Institute, National Research Council, via Madonna del Piano, 10, 50019 Florence, Italy
[4]Department of Biology & Biotechnology 'Lazzaro Spallanzani', University of Pavia, Via Ferrata 9, 27100 Pavia, Italy
[*]Author for correspondence: Tel.: +39 055 457 4742 ■ Fax: +39 055 228 8250 ■ renato.fani@unifi.it
[‡]Authors contributed equally

Aim: The aim of this work was to analyze the eight resistance–nodulation–cell division (RND) families (a group of proteins mainly involved in multidrug resistance of Gram-negative bacteria) in 26 *Burkholderia* genomes in order to gain knowledge regarding their presence and distribution, to obtain a platform for future experimental tests aimed to identify new molecular targets to be used in antimicrobial therapy against *Burkholderia* species and to refine the annotation of RND-like sequences in these genomes. **Materials & methods:** A total of 417 coding sequences were retrieved and analyzed using different bioinformatics tools. **Results & conclusion:** A complex pattern of RND presence and distribution in the different *Burkholderia* species was disclosed and a core of proteins represented in all 26 genomes was identified. These 'core' proteins might represent useful targets of new synthetic antimicrobial compounds. Furthermore, the annotation of RND-like sequences in *Burkholderia* was refined.

The resistance–nodulation–cell division (RND) superfamily includes proteins that are found ubiquitously in bacteria, Archaea and eukaryotes [1–3].

All characterized members of this superfamily potentially catalyze substrate efflux via an H^+ antiport mechanism [3]. Most of these transport systems consist of a polypeptide chain of variable length of 700–1300 amino acid residues. The structure of these proteins can be split into 14 regions:

- A transmembrane segment (TMS) at their N-terminus;
- An extracytoplasmic domain;
- Six TMSs;
- Another extracytoplasmic domain;
- Five final C-terminal TMSs.

Most RND proteins consist of a single polypeptide chain [3]. The first and second halves of RND proteins share a high degree of sequence similarity, suggesting that the encoding genes result from a gene elongation event [4] of an ancestral gene half the size of the extant gene that probably occurred in the primordial system prior to divergence of the family members. Some archaeal and eukaryotic RND homologs are half the size and have no internal duplication [3].

Functionally characterized RND members fall into eight different families exhibiting a different phylogenetic distribution. Four of them are scattered through different taxa, while the other four are restricted to Gram-negative bacteria and have different substrate specificity: one being responsible for the export of multiple drugs (HAE-1); one catalyzing heavy metal efflux (HME); and one probably catalyzing the export of lipooligosaccharides concerned with plant nodulation for symbiotic nitrogen fixation (putative NFE) [3]. The fourth Gram-negative family, the aryl polyene pigment exporters (APPEs), is very distantly related to the other established members of the superfamily, and its members were identified as a pigment exporter in *Xanthomonas oryzae* [5].

The RND members of the first three Gram-negative families form protein complexes by a RND protein in the cellular membrane, an outer membrane protein (OMP) and a periplasmic-located membrane adaptor protein (belonging to the membrane fusion protein [MFP] family), which connects the other two proteins [3]. These complexes use proton-motive force to bind different substrates, either from the periplasm and/or the cytoplasm, and cause them to be extruded. The genes coding for these proteins are usually arranged in an operon. The MFP and RND coding genes are often cotranscribed [6];

Keywords
■ antibiotic resistance ■ *Burkholderia* ■ efflux pumps ■ genomics ■ new antibiotics ■ RND

Future Medicine part of fsg

however, in some systems and/or Gram negative species, the OMP is not linked to the MFP and RND encoding genes [7,8].

The HAE-1 family is the best known of all the eight families, as its representatives are one of the main determinants of multidrug resistance in Gram-negative bacteria [9–11]. These proteins have been extensively studied in several microorganisms [12,13]. In particular, AcrB from *Escherichia coli* and MexB from *Pseudomonas aeruginosa* (and the associated MFP and OMP proteins) are the best known RND drug transporters in bacteria and have served as the prototypes for biochemical and structural studies of such pumps [14–20].

The HME family includes proteins involved in heavy-metal efflux. Unlike the HAE-1 family, members of the HME family have high substrate specificity, discerning between monovalent and divalent ions [21]. Recently, the crystal structure of the three components of a complex belonging to this family, the *E. coli* CusABC, was obtained [21–24].

The representative protein of the NFE family is NolG, a putative nodulation factor exporter in rhizobia that probably functions in association with the product of the neighboring gene *nolF* (MFP family) [1,2,25]. Recently, homologs of these proteins have been identified in the genome sequences of many other bacteria [26].

The SecDF proteins can be found in both bacteria and Archaea [2,27,28]. It has been shown that the *E. coli secDF* genes are organized in an operon also containing the *yajC* gene [29]. They form a membrane protein complex that interacts in a transient fashion with the Sec translocon (the major facilitator in the translocation and insertion of proteins across or into the inner membrane of prokaryotes) and stimulates preprotein translocation [30]. Although SecD and SecF are not essential for cell life, their inactivation in *E. coli* results in a severe pleiotropic protein secretion defect, as well as severe growth inhibition and a cold-sensitive phenotype [2,30]. The crystal structure of *Thermus thermophilus* SecDF was obtained in 2011 [31]. In *Staphylococcus aureus*, it has also been demonstrated that the *secDF* deletion has a combination of different effects on transcription, regulation and translocation, leading to impaired cell division, reduced resistance and altered expression of virulence determinants. This suggests that SecDF might be of major importance in *S. aureus* [32].

The HAE-2 family comprises members exclusively from Gram-positive bacteria [2] and only a few representatives of this family have been studied [3]. In the *Mycobacterium tuberculosis* genome, 13 putative RND-type transporters were identified and defined as mycobacterial membrane proteins, large, or MmpL. It has been shown that drug susceptibility was not altered by the inactivation of 11 of these 13 genes [33]. Nevertheless, the expression of MmpL7 in *Mycobacterium smegmatis* confers a high-level resistance to isoniazid to the cell. Accordingly, the presence of efflux pump inhibitors causes a decrease of the resistance level [13,33]. Recently, it has also been demonstrated that MmpL3 is the cellular target of the antitubercular pyrrole derivative BM212 [34].

The HAE-3 family comprises members from both Archaea and Spirochaete. The proteins included in this family were revealed by genome sequencing. The function performed by these proteins has not yet been investigated [2,3].

Some or all of the eukaryotic proteins may function in cholesterol/steroid hormone transport, reception, regulation and catalysis [3]. Examples of proteins belonging to this family are Ptc, Disp, membrane-bound NPC1 and water-soluble NPC1 and NPC2 [2,35,36].

Finally, one group of RND proteins has been termed hopanoid biosynthesis-associated RND transporters or HpnN [35]. Hopanoids are pentacyclic triterpenoids that may be surrogates for eukaryotic sterols in bacteria [37]. The *hpnN* genes are associated with hopanoid biosynthesis genes in many bacterial genomes [38]. It is unclear whether these proteins are actually involved in hopanoid transport; it seems true for *Rhodopseudomonas palustris* TIE-1 [38], but not for *Burkholderia cenocepacia* [37]. Moreover, the assignment of this subfamily to the RND superfamily is not entirely clear: they seem related to the APPE and HAE-3 family [38], but some authors argue that the eukaryotic RND transporters arose from this particular group of proteins [35]. Remarkably these proteins are involved in antibiotic resistance in some *Burkholderia* strains [37,39].

The *Burkholderia* genus is an interesting and complex bacterial taxonomic unit that includes a variety of species (some of which are pathogenic) inhabiting different ecological niches, including plants and animals [40,41]. Representatives of some of these species interact at different levels with plants; for example, *Burkholderia glumae* is a phytopathogenic species responsible for seedling and grain rot in rice, and wilting symptoms in different plant species [40]; *Burkholderia phymatum* is involved in plant nodulation [40]; and another strain (*Burkholderia* sp. 1002), able to fix nitrogen, has been isolated from a *Mimosa occidentalis* nodule

[42]. The deep interaction between *Burkholderia* species and plants is remarked also by *Burkholderia phytofirmans*, an endophytic species that provides useful benefits to the host plants [40] and by an intracellular symbiont of a phytopathogenic fungus, *Burkholderia rhizoxinica* [43]. The exceptional metabolic plasticity exhibited by bacteria belonging to the *Burkholderia* genus is also highlighted by the existence of species able to degrade pollutants, such as *Burkholderia xenovorans* [40], and also by the ability of many species to interact with animals and humans. Indeed, *Burkholderia mallei* and *Burkholderia pseudomallei* are the etiological agents of glanders and melioidosis, respectively; and it has been demonstrated that *Burkholderia gladioli*, *Burkholderia fungorum* and all *Burkholderia cepacia* complex (Bcc) bacteria represent opportunistic pathogens in humans [41]. The latter is a heterogeneous group embedding (at least) seventeen genetically distinct, but phenotypically similar species [40,44–46]. They are important opportunistic pathogens that infect the airways of cystic fibrosis patients. The eradication of human *Burkholderia* infections is particularly difficult owing to the high antibiotic resistance of these bacteria [47,48], and their multidrug resistance is due to the presence of RND proteins, among other factors [49–55].

In a previous study, we investigated the presence and distribution of two RND protein families, HAE-1 and HME, in 21 completely sequenced *Burkholderia* genomes [56]. This work revealed a complex pattern of gene copy number, organization and phylogentic distribution. In the present work we aim to extend the analysis to all eight families of RND superfamily in 26 completely sequenced *Burkholderia* genomes to obtain knowledge regarding the presence and distribution of this protein group. We aimed to obtain a valuable platform for future experimental tests aimed at identifying new molecular targets for antimicrobial therapy against *Burkholderia* species, and to refine the annotation of RND-like sequences in these 26 *Burkholderia* genomes.

Materials & methods

Sequence retrieval

Amino acid sequences from the 26 completely sequenced genomes of *Burkholderia* representatives (as of 31 March 2011) were retrieved from the GenBank database [101] (Table 1). BLAST probing of the database was performed with the BLASTP algorithm using default parameters [57]. Only those sequences retrieved at an E-value lower than 0.05 were taken into account.

Amino acid sequences of experimentally characterized RND proteins were retrieved from the Transport Classification Database (TCDB) [58,59,102]. Amino acid sequences of putative NFE and APPE proteins were retrieved from the protein section at the National Center for Biotechnology Information (NCBI) database [103].

Sequence alignment

Multiple amino acid sequence alignments were performed using the Muscle [60] and the MAFFT program [61], and the alignments were visually reviewed in order to remove misaligned regions.

Phylogenetic analysis

The Mega5 program [62] was used for the construction of neighbor-joining phylogenetic trees, using the pairwise deletion option and 1000 bootstrap replicates.

The concatamer shown in Figure 1 was obtained adopting the following procedure:

- The orthologs of *atpD* (BCAL0036), *gltB* (BCAL0289), *gyrB* (BCAL0421), *recA* (BCAL0953), *lepA* (BCA1003), *phaC* (BCAL1861) and *trpB* (BCAM0991; with gene numbers of the *B. cenocepacia* strain J2315), were retrieved from each of the *Burkholderia* genomes;
- Each ortholog dataset was independently aligned;
- All the different multialignments were concatenated into a single one comprising 5068 residues.

Hydropathy plot

Hydropathy plots were obtained using two different programs:

- Protscale [63] on the ExPASy website [104], using the Kyte and Doolittle scale [64], a window size of 19 and other default parameters;
- Average Hydropathy, Amphipathicity and Similarity (AveHAS) [65] on the TCDB website [102] using default parameters.

Prediction of transmembrane regions

Prediction of transmembrane regions was obtained using two different programs:

- TMHMM Server v. 2.0 [66,67] on the ExPASy website [104];
- AveHAS [65] on the TCDB website [102] using default parameters.

Table 1. Characteristics of the 26 *Burkholderia* genomes analyzed.

Species	Strain	Genome size (Mbp)	Chromosomes	Plasmids
Burkholderia ambifaria	AMMD	752,856	3	1
B. ambifaria	MC40–6	764,094	3	1
Burkholderia cenocepacia	AU 1054	727,911	3	0
B. cenocepacia	HI2424	771,542	3	1
B. cenocepacia	J2315	804,308	3	1
B. cenocepacia	MC0–3	795,748	3	0
Burkholderia glumae	BGR1	726,736	2	4
Burkholderia mallei	ATCC_23344	582,538	2	0
B. mallei	NCTC_10229	575,821	2	0
B. mallei	NCTC_10247	585,269	2	0
B. mallei	SAVP1	523,492	2	0
Burkholderia lata	383	868,708	3	0
Burkholderia multivorans	ATCC_17616	701,139	3	1
Burkholderia phymatum	STM815	867,919	2	2
Burkholderia phytofirmans	PsJN	821,354	2	1
Burkholderia pseudomallei	1106a	710,000	2	0
B. pseudomallei	1710b	730,805	2	0
B. pseudomallei	668	702,746	2	0
B. pseudomallei	K96243	724,755	2	0
Burkholderia rhizoxinica	HKI_454	379,000	1	2
Burkholderia sp.	CCGE1001	690,000	2	0
Burkholderia sp.	CCGE1002	789,000	3	1
Burkholderia sp.	CCGE1003	710,000	2	0
Burkholderia thailandensis	E264	671,477	2	0
Burkholderia vietnamiensis	G4	839,182	3	5
Burkholderia xenovorans	LB400	973,530	3	0

Search for protein families, domains, regions & sites

The search for protein families, domains, regions and sites was performed, with default parameters, using two different tools:

- The CD-Search against the NCBI's Conserved Domain Database (CDD) [68,69] at the NCBI website [105].
- InterProScan sequence search against the InterPro database [70,106].

Results & discussion

Identification & distribution of putative RND genes in the *Burkholderia* genus

In a previous work [56], we identified 254 putative RND-coding sequences in 21 completely sequenced *Burkholderia* genomes, using the experimentally characterized RND protein CeoB (gene identifier: 206564391 *B. cenocepacia* J2315, HAE-1 family) as the BLAST [57] seed. This was obtained by:

- A deep phylogenetic analysis;
- An *in silico* comparison with experimentally characterized HAE-1 and HME proteins belonging to other microorganisms;
- An analysis of highly conserved residues involved in proton translocation and substrate recognition. We assigned the majority of these sequences to HAE-1 and HME families. Only for a cluster of proteins (defined as uncertain function [UF]), was it not possible to establish the family they belonged to.

Despite different draft genomes being present in the database at the time of our analysis, we preferred to focus on only completely sequenced

	HAE-1	HME	UpF	SecDF	HpnN	PutativeAPPE	Cluster 27	Cluster 29	Cluster 30	Cluster 31	Total number of RNDs
B_cenocepacia_AU1054	12	2	3	2	1	1	0	0	0	1	22
B_cenocepacia_H2424	13	2	3	2	1	1	0	0	0	1	23
B_cenocepacia_MCO_3	13	2	3	2	1	0	0	1	0	1	23
B_cenocepacia_J2315	11	2	3	2	1	1	0	0	1	1	22
B_lata_383	11	1	1	2	1	1	0	0	1	2	20
B_ambifaria_AMMD	7	1	3	2	1	1	1	0	0	0	16
B_ambifaria_MC40_6	9	1	3	2	1	1	1	0	0	0	18
B_vietnamiensis_G4	9	1	1	2	1	1	1	0	0	0	16
B_multivorans_17616	8	3	1	2	1	0	0	0	0	1	16
B_mallei_ATCC23344	5	2	0	2	1	0	0	0	0	0	10
B_mallei_NTCT10229	4	2	0	2	1	0	0	0	0	0	9
B_mallei_NCTC10247	4	2	0	2	1	0	0	0	0	0	9
B_mallei_SAVP1	4	2	0	2	1	0	0	0	0	0	9
B_pseudomallei_668	8	2	0	2	1	0	0	0	0	0	13
B_pseudomallei_K96243	8	2	0	2	1	0	0	0	0	0	13
B_pseudomallei_1710b	8	2	0	2	1	0	0	0	0	0	13
B_pseudomallei_1106a	8	2	0	2	1	0	0	0	0	0	13
B_thailandiesis_E264	9	2	0	2	1	0	0	0	0	0	14
B_glumae_BGR1	9	0	1	2	1	0	0	0	0	0	13
B_sp_CCGE1001	9	0	2	2	1	0	1	0	0	0	15
B_sp_CCGE1003	7	1	2	2	1	0	1	1	0	0	15
B_phytofirmans_PsJN	12	1	3	2	1	0	1	0	0	0	20
B_xenovorans_LB400	11	1	5	2	1	0	1	1	0	0	22
B_sp_CCGE1002	15	1	3	2	1	0	1	1	0	1	25
B_phymatum_STM815	14	0	2	2	1	0	1	0	0	1	21
B_rhizoxinica_HKI454	4	0	0	2	1	0	0	0	0	0	7
Total	**232**	**37**	**39**	**52**	**26**	**7**	**9**	**4**	**2**	**9**	

Figure 1. Phylogenetic tree based on the concatenated sequences of seven housekeeping genes and table of distribution of resistance–nodulation–cell division proteins in each genome.
APPE: Aryl polyene pigment exporter; HME: Heavy metal efflux; RND: Resistance–nodulation–cell division.
Data taken from [79].

genomes in order to avoid misinterpretation of data, since draft genomes do not provide robust information when searching for gene presence/absence patterns and/or genomic structure features. In particular, our dataset consists of the 26 completely sequenced *Burkholderia* genomes available at the NCBI database (as of 31 March 2011) and listed in Table 1, including strains belonging to species with a different origin and with different metabolic abilities.

To check the distribution of all RND protein families in these 26 completely sequenced *Burkholderia* genomes, we used several approaches, summarized in Figure 2. First, we extended our previous analyses (only HAE-1 and HME families) to five additional complete genomes, namely *B. glumae* BGR1, *B. rhizoxinica* HKI_454, *Burkholderia* sp. CCGE1001, *Burkholderia* sp. CCGE1002 and *Burkholderia* sp. CCGE1003, using the *B. cenocepacia* J2315 CeoB amino acid sequence as a BLAST [57] seed (see 'Material & methods' section). A total of 54 sequences were retrieved.

Second, to check the presence of proteins belonging to the other RND families, we retrieved the 24 experimentally characterized sequences representative of all the other RND families from the TCDB (Supplementary File 1; see online at www.futuremedicine.com/doi/suppl/10.2217/fmb.13.50) [58,59,102]. Each of them was used as a query to probe the 26 *Burkholderia* genomes, using default parameters (see 'Material & methods' section) and performing an extensive, reiterative BLAST search. A preliminary phylogenetic analysis was performed on these sequences (data not shown) and all the sequences that fell within the same cluster in the obtained phylogenetic tree were grouped together, and a sequence representative of each cluster was used as a probe for a further BLAST analysis to avoid the exclusion of other putative RND sequences owing to their phylogenetic distance from the sequences embedded in the TCDB. All the sequences retrieved were compared with those previously identified, to prevent any redundancy. Using this method, a total of 417 putative RND sequences were collected. A highly variable number of sequences, ranging from seven (in *B. rhizoxinica* HKI454) to 25 (in *Burkholderia* sp. CCGE1002) was detected in the different genomes. Since eukaryotic sequences are very divergent from those of *Burkholderia*, and they did not give statistically significant results in the BLAST analysis, they were excluded from further analyses.

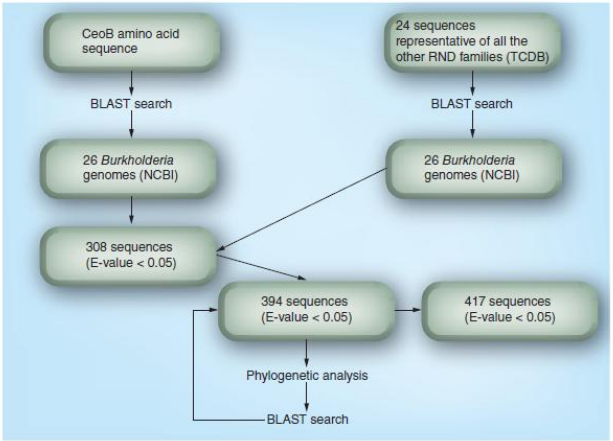

Figure 2. Flowchart of the bioinformatics analysis performed for searching resistance–nodulation–cell division like-sequences.
NCBI: National Center for Biotechnology Information; RND: Resistance–nodulation–cell division; TCDB: Transport Classification Database.

Phylogenetic analysis of the 417 RND *Burkholderia* sequences

The 417 RND-like sequences obtained from the BLAST analysis were aligned and the multialignment obtained was used to build the phylogenetic tree reported in Supplementary File 2. All the sequences falling within the same cluster were grouped together to obtain the tree reported in Figure 3, where each black triangle corresponds to a specific cluster of sequences. To facilitate the interpretation of the results, the various clusters have been labeled with different numbers (from 1 to 32).

Moreover, 57 sequences representative of all the RND families retrieved from the TCDB (excluding the eukaryotic sequences, see Supplementary File 1) were added to the aforementioned multialignment to obtain a first indication of the family to which each cluster belongs to. The multialignment obtained was used to build the phylogenetic tree reported in Supplementary File 3. In this tree, some of the 417 *Burkholderia* sequences are grouped into clusters that also included sequences of the characterized proteins retrieved from the TCDB, thus showing similarity with them and giving a first indication of the possible family they belong to. However, several other sequences fall in clusters that show no similarity with TCDB sequences. Accordingly, each cluster was analyzed individually.

HAE-1, HME & UF (clusters 1–24)

Sequences included in clusters 1–10, 13 and 17–24 probably belong to the HAE-1 family, while sequences in clusters 11 and 12 probably belong to the HME family. Indeed, most of these sequences were previously (*in silico*) characterized [56] by a deep phylogenetic analysis: comparison with experimentally characterized HAE-1 and HME proteins belonging to other microorganisms and the analysis of highly conserved residues involved in proton translocation and substrate recognition. Sequences identified in the additional five *Burkholderia* genomes were assigned to these families because they fell in the same clusters previously identified. For further confirmation, motives and residues characteristic of these two families [56] were analyzed, confirming their correct affiliation (data not shown). Moreover some of the clusters affiliated to the HAE-1 family include examples of published *Burkholderia* efflux pumps involved in antibiotic resistance. In particular AmrB [54], BpeB [55] and BpeF [71] of *B. pseudomallei* are included in clusters 3, 4 and 10, respectively, and cluster 10 also includes CeoB of *B. cenocepacia* [52].

Sequences embedded in clusters 14–16 were previously defined as UF [56] because they could not be assigned to any RND family. This (more extensive) analysis confirms previous data since they show no similarity with any sequence belonging to characterized RND families. As shown in Figure 3, they fall into a larger cluster that includes all RND sequences whose genes are associated in an operon with MFP and OMP genes (HAE-1, HME and NFE families).

Concerning the NFE family, only one sequence has been characterized [3]. Therefore, to more thoroughly investigate the possible affiliation of UF sequences, we retrieved 81 additional putative NFE sequences from the protein section of the NCBI website [103]. Since none of these sequences have been experimentally characterized, they were aligned with all RND sequences retrieved from the TCDB database (excluding the eukaryotic sequences) to verify that they belong to NFE family, not to other RND families. The multialignment obtained was used to build a phylogenetic tree (data not shown), which revealed that only 42 of these sequences clustered with the NFE sequence, whereas the others joined other RND family sequences. These 42 sequences were used for further analysis. They have a different phylogenetic distribution, although most of them belong to Proteobacteria. Following this, the 42 sequences were aligned to the 417 putative RND *Burkholderia* sequences and the multialignment obtained was used to build the phylogenetic tree reported as Supplementary File 4. This tree shows that all the 42 putative NFE sequences grouped in the same cluster, which did not include any *Burkholderia* sequence. The whole body of data obtained confirmed that, although UF sequences joined a larger cluster including HAE-1, HME and NFE sequences, they apparently do not belong to any of these families. This is also in agreement with the analysis of the gene triad coding for RND, MFP and OMP. Indeed we found that the genes are apparently organized in an operon independently from the function performed (HAE-1, HME or UF). Genes belonging to the same family share the same operon organization, but genes belonging to different families (HAE-1, HME or UF) exhibited a different relative gene order. Aside from the intriguing question of how the operon organization is correlated to the function performed (an issue that is beyond the scope of the present work), the presence of the different operon organization and the fact that the sequences with UF showed no similarity to any

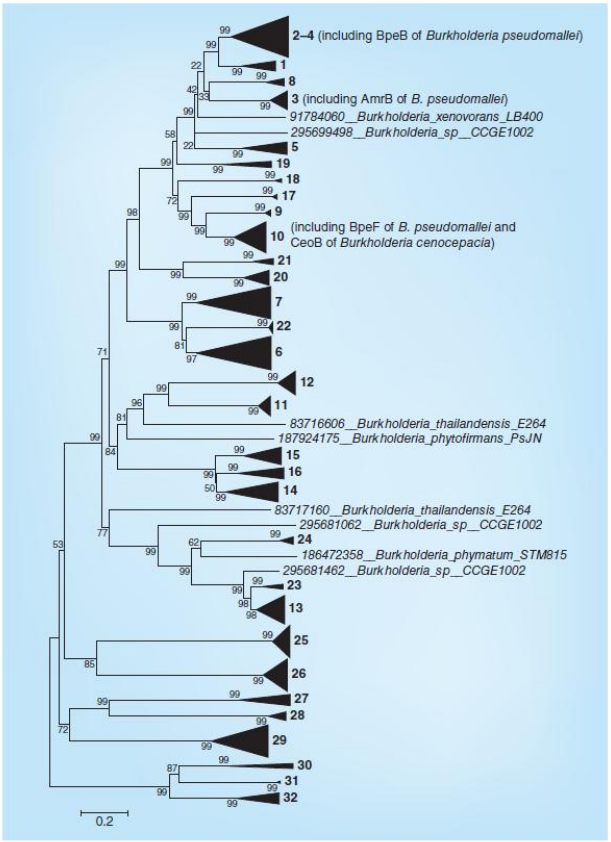

Figure 3. Phylogenetic tree constructed using the 417 *Burkholderia* putative resistance–nodulation–cell division sequences. The entire phylogentic tree is given in Supplementary File 2. In this schematic figure, all the sequences falling within the same cluster were grouped together and represented by a black triangle. To facilitate the interpretation of the results, the various clusters have been labeled with different numbers (from 1 to 32).

known RND proteins, suggests that they might belong to a new and not yet characterized RND family. Experimental analyses are in progress to determine the substrate transported by these proteins and to infer their role in *Burkholderia* representatives.

SecDF (clusters 25 & 26)

Sequences in clusters 25 and 26 were assigned to SecF and SecD, respectively. The assignment of these sequences to the SecDF family was based on three lines of evidence, the first being the similarity with SecD and SecF representatives

shown on the phylogenetic tree reported in Supplementary File 3. Additionally, each sequence was used as a query for a BLAST probing in the NCBI database, using default parameters, and for a search of conserved domains at NCBI's CDD. Both analyses unambiguously identified these sequences as SecD and SecF proteins. Finally, we found the presence of two signature sequences (one for SecD proteins and one for SecF) and some conserved residues previously identified by [2] as typical of SecDF proteins (data not shown). One copy of *secD* and one of *secF* are present in all 26 *Burkholderia* genomes analyzed. In *E. coli* these two genes are associated in an operon that also contains the *yajC* gene [29]. The same operon organization is found in all the *Burkholderia* genomes analyzed (an example is reported in Figure 4). This operon is always located on chromosome 1, with an average identity at amino acid level of 87% for SecD sequences and 91% for SecF among the *Burkholderia* genus, revealing a high degree of sequence conservation throughout the genus.

Putative APPE (cluster 28)

In the phylogenetic tree reported in Supplementary File 3, sequences of cluster 28 are grouped with a sequence belonging to the APPE family (ORF4 in the pigment gene locus of *X. oryzae* pv. *oryzae* [Q9EY29], see Supplementary File 1). Only this experimentally characterized sequence representative of the APPE family is available from the TCDB database. Therefore, to more thoroughly investigate the possible affiliation of sequences included in cluster 28 to this family, we retrieved 31 additional putative APPE sequences from the NCBI website [101]. All these sequences belong to γ-proteobacteria and have been assigned only on the basis of sequence homology. Since none of the sequences has been experimentally characterized, we performed additional analyses to verify whether they all belong to the APPE family, as opposed to other RND families. Specifically, they were aligned with all RND sequences retrieved from the TCDB database (excluding the eukaryotic sequences) and the obtained multialignment was used to build a phylogenetic tree (data not shown) in which all the 31 sequences grouped together in a monophyletic cluster that also included the *X. oryzae* pv. *oryzae* sequence belonging to TCDB, confirming that they likely belong to this family.

Following this, the 31 sequences were aligned with the 417 putative RND *Burkholderia* sequences and the multialignment obtained was used to build the phylogenetic tree reported in Supplementary File 5. In this tree, sequences of cluster 28 fall in the same cluster as the 31 putative APPE sequences, supporting the idea that they might belong to the APPE family.

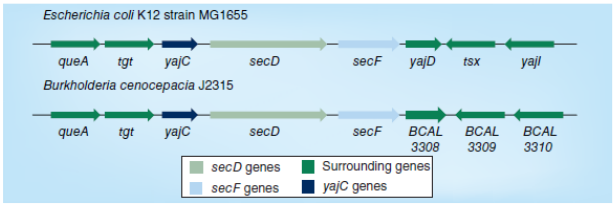

Figure 4. Schematic representations of the organization of the *secDF* operon in *Escherichia coli* K12 strain MG1655 and *Burkholderia cenocepacia* J2315. The organization of the genes (*secD*, *secF*, *yajC* and surrounding genes) identified in *Escherichia coli* K12 strain MG1655 and *Burkholderia cenocepacia* J2315 [107] are depicted. In the *E. coli* K12 strain MG1655 genome: *queA*: S-adenosylmethionine:tRNA ribosyltransferase-isomerase (locus tag b0405); *tgt*: tRNA-guanine transglycosylase (locus tag b0406); *yajC*: SecYEG protein translocase auxillary subunit (locus tag b0407); *secD*: SecYEG protein translocase auxillary subunit (locus tag b0408); *secF*: SecYEG protein translocase auxillary subunit (locus tag b0409); *yajD*: conserved protein, HNH family (locus tag b0410); *tsx*: nucleoside channel, receptor of phage T6 and colicin K (locus tag b0411); *yajI*: predicted lipoprotein (locus tag b0412). In the *B. cenocepacia* J2315 genome: *queA*: S-adenosylmethionine:tRNA ribosyltransferase-isomerase (locus tag BCAL3303); *tgt*: putative queuine tRNA-ribosyltransferase (locus tag BCAL3304); *yajC*: preprotein translocase subunit YajC (locus tag BCAL3305); *secD*: preprotein translocase subunit SecD (locus tag BCAL3306); *secF*: preprotein translocase subunit SecF (locus tag BCAL3307); *BCAL3308*: putative peptidase (locus tag BCAL3308); *BCAL3309*: major facilitator superfamily protein (locus tag BCAL3309); *BCAL3310*: hypothetical protein (locus tag BCAL3310). For color images please see online www.futuremedicine.com/doi/pdf/10.2217/fmb.13.50.

Unknown proteins (clusters 27, 29, 30, 31 & 32)

Sequences included in clusters 27, 29, 30, 31 and 32 did not join any of the TCDB sequences. Therefore, in order to check if they are actually RND proteins and to attempt to decipher their function in the cell, we performed different types of analyses. First, the conservation of RND protein structure by hydropathy plot analysis and the prediction of transmembrane regions was assessed. Hydropathy plots were obtained using two different programs and comparing the results: Protscale [63] on the ExPASy website [104], and AveHAS [65] on the TCDB website (see 'Materials & methods' section) [102]. In addition, for the prediction of transmembrane regions we used different programs: TMHMM Server v. 2.0 [66,67] on the ExPASy website [104] and AveHAS.

The hydropathy plot analysis and the prediction of transmembrane regions revealed the presence of the 12 TMSs and of the two large loops characteristic of RND proteins in all the sequences included in these five clusters with all the programs used for the analysis. These data confirm the conservation of RND protein structure. The entire set of data is reported as Supplementary File 6.

Furthermore, an analysis to identify conserved domains, regions and sites within these unclassified sequences was performed. To this purpose, two different tools were used: the CD-Search against the NCBI's CDD [68,69], and InterProScan sequence search against the InterPro database [70].

The analysis of conserved domains affiliated sequences of cluster 29 to HpnN, the group of RND proteins that are associated with hopanoid biosynthesis genes in many bacterial genomes [38]. One copy of this sequence is present in each of the 26 *Burkholderia* genomes analyzed; moreover, in their physical proximity, other genes involved in hopanoid biosynthesis are often found. The number and the type of genes involved in this process and associated with these RND transporters varied depending on the *Burkholderia* genome analyzed; however, the gene coding for Shc, which is essential for hopanoid biosynthesis [37], is present in all the 26 genomes.

Sequences included in the other four clusters (27, 30, 31 and 32) were classified as transporters and both programs used localized these proteins on the cytoplamatic membrane (see Supplementary File 7). Their putative transmembrane regions have statistically significant similarities with the transmembrane regions of RND proteins belonging to different families, whereas the regions corresponding to the hypothetical periplasmatic loops showed no similarity to any known domain present in the databases. In particular, sequences of clusters 30, 31 and 32 have statistically significant similarity along the entire sequence with HAE-3 proteins, but no further evidence to classify them as belonging to this family was found.

Many studies [72–77] have demonstrated that the periplasmic regions of RND proteins are involved in substrate recognition. Thus, the fact that the regions corresponding to the hypothetical periplasmatic loops showed no similarity to any known domain present in the database, although the overall structure characteristic of RND proteins is conserved, might be related to the type of substrate they transport, which is not known/characterized yet. To obtain hints on their possible function, genes located around each of these sequences were analyzed to test whether the genes encoding these transporters are placed in clusters embedding genes involved in a particular metabolic process. However, this analysis did not give any significant results.

Figure 5 reports the phylogenetic tree showing the RND clustering on the basis of their putative function suggested by the previously described analyses. The analysis of Figure 5 revealed that the majority of sequences retrieved were assigned to the HAE-1 family, which are grouped together in a cluster; there are also two embedding clusters of sequences affiliated to the HME family and of the putative new family (UF). The topology of the tree reported in Figure 5 is in full agreement with a previous phylogenetic study of the RND superfamily [78], revealing that sequences belonging to the HME and NFE families form two clusters that are embedded in a larger HAE-1 sequence group. It is worth noting that in *Burkholderia* we did not find any sequence representative of the NFE family; however, the putative new family formed by UF sequences occupies the same position of NFE sequences in the tree reported by [78]. This raises the intriguing question of the function performed by the UF proteins, since the *in silico* analysis performed in this work has shown that these proteins do not belong to NFE family.

Sequences belonging to the SecDF family branch from a central position in the tree, separating two major branches, one (top) mentioned previously and the other that, in the work of Yen *et al.*, consists of the EST, HAE-2, HAE-3 and APPE family proteins, whereas in our

work consists of the putative APPE and HpnN sequences and of clusters 27, 30, 31 and 32 [78].

Distribution of RND-coding genes

To assess the relationship between the number of putative RND proteins of each individual group in each genome analyzed and the taxonomy of these species, a phylogenetic tree was constructed from the alignment of the concatened sequences of seven housekeeping genes [79], which are used for the multilocus sequence analysis of Bcc species [79], the most effective way to discriminate between these very similar species to date [80]. In Figure 1, the tree showing the phylogenetic relationship between the 26 *Burkholderia* analyzed is reported, along with the number of RND genes per family. The analysis of data reported in Figure 1 revealed a complex pattern of phylogenetic distribution of each family/sequence:

- Sequences belonging to HAE-1 family are present in all 26 genomes, with a different number of homologs (ranging from 4 in *B. rhizoxinica* HKI454 to 15 in *Burkholderia* sp. CCGE1002) and are the most abundant in all 26 genomes;
- One copy of *secD* and one copy of *secF* are present in each genome;
- One copy of *hpnN* is present in all 26 of the genomes;
- At least one copy of sequences belonging to the HME family are present in 22 genomes;
- Putative APPE sequences are present only in strains belonging to Bcc;
- In the cluster that includes *B. mallei*, *B. pseudomallei* and *B. thailandiensis* strains, only sequences of HAE-1, HME and SecDF families, and HpnN transporters are present;
- Sequences belonging to clusters 27, 30, 31 and 32 showed a scattered distribution.

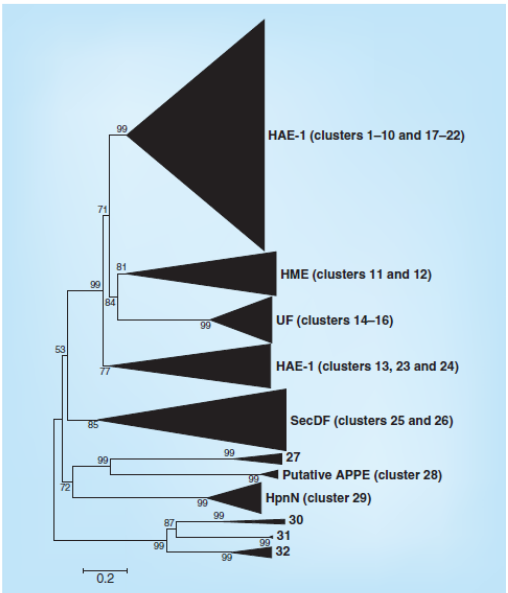

Figure 5. Phylogenetic tree constructed using the 417 *Burkholderia* putative resistance–nodulation–cell division sequences.
APPE: Aryl polyene pigment exporter; HME: Heavy metal efflux.

Conclusion

In this work, we have performed a comprehensive comparative analysis of the RND superfamily efflux systems in 26 completely sequenced *Burkholderia* genomes. A total of 417 coding sequences were retrieved from these genomes and analyzed at different levels, adopting different bioinformatics tools. This allowed the assignment of a putative function to the majority of them.

A total of 232 sequences have been assigned to the HAE-1 family, involved in antibiotic resistance, 37 sequences were affiliated to the HME family (heavy-metal efflux) and 39 sequences fell in a cluster that probably represents a new and not yet characterized RND family (UF). Experimental analyses are in progress to determine the substrates transported by these proteins and to try to determine their role in the *Burkholderia* genus.

One copy each of *secD* and *secF* are present and highly conserved in all the genomes analyzed. In addition, one copy of the putative hopanoid transporter HpnN is present in all 26 *Burkholderia* genomes and this gene is always associated with the *SHC* gene that is essential for hopanoid biosynthesis [37]. A group of putative APPE proteins was identified and only 24 sequences (divided into four different clusters, 27, 30, 31 and 32) were not assigned to any RND family and, although they retain the characteristic structure of the RND proteins, it has not been possible to obtain any information regarding their function.

The phylogentic tree reported in Figure 5 and obtained on the basis of the alignment of the 417 *Burkholderia* sequences is consistent with the phylogenetic analysis of the RND superfamily [78].

The relationship between the number of putative RND proteins of each group identified in each genome analyzed and the taxonomy of these species was also analyzed. The finding that at least one copy of the genes belonging to the HAE-1 and SecDF families and to HpnN trasporters is present in all the genomes analyzed (including *B. rhizoxinica* HKI454, which is an intracellular symbiont of a phytopathogenic fungus and has undergone a drastic genome reduction [43]), represents an interesting issue from different viewpoints. From an evolutionary perspective, this strongly suggests that its presence might be conserved throughout the *Burkholderia* genus and, therefore, might be present in the genome of the *Burkholderia* ancestor. From a functional viewpoint, this finding strongly suggests that these proteins might play an important, if not essential, role in these bacteria. Even though the function that they have in the natural environment is yet to be clearly elucidated, it is known that these proteins are involved in the extrusion of different antimicrobial and/or toxic compounds in different microorganisms [9–11,32,37,39] rendering them resistant to these molecules. Accordingly, they might represent good putative targets for new synthetic antibiotic molecules. These data may serve as a solid basis for future experimental tests aimed at verifying their possible use in antimicrobial therapy against *Burkholderia* species.

Finally, the analyses performed in this work allowed refinement of the genome annotation of the 26 *Burkholderia* genomes analyzed. Indeed, nowadays, we found ourselves in the paradoxal situation in which the more sequences we obtain, the less we known about them. The accurate analyses performed in this work allow improvement of the accuracy of gene annotation usually carried out in an automatic fashion, which is based on superficial sequence homology analysis.

Financial & competing interests disclosure

This work was supported by the Italian Cystic Fibrosis Research Foundation (FFC project 10#2012) and Ente Cassa di Risparmio (Grant 2008.1103). M Fondi is financially supported by a FEMS Advanced Fellowship (FAF2012). The authors have no other relevant affiliations or financial involvement with any organization or entity with a financial interest in or financial conflict with the subject matter or materials discussed in the manuscript apart from those disclosed.

No writing assistance was utilized in the production of this manuscript.

Ethical conduct of research

The authors state that they have obtained appropriate institutional review board approval or have followed the principles outlined in the Declaration of Helsinki for all human or animal experimental investigations. In addition, for investigations involving human subjects, informed consent has been obtained from the participants involved.

Executive summary

The resistance–nodulation–cell division superfamily

- The resistance–nodulation–cell division (RND) superfamily consists of a group of proteins that are spread ubiquitously in all organisms. They appear to have become particularly established in the Gram-negative bacteria, where they are a major cause of multidrug resistance.
- This superfamily is divided into eight different families, four of which are only present in Gram-negative bacteria.
- Little is known about the presence of these proteins in the *Burkholderia* genus.

Aims of the study

- In this work we aim to analyze all eight families of RND superfamily in 26 *Burkholderia* completely sequenced genomes to obtain knowledge of the presence and distribution of this protein group.
- We aimed to obtain a valuable platform for future experimental tests aimed to identify new molecular targets to be used in antimicrobial therapy against *Burkholderia* species and to refine the annotation of RND-like sequences in these 26 *Burkholderia* genomes.

Conclusion

- We gained knowledge regarding the presence and distribution of RND proteins group in the *Burkholderia* genus.
- A core of proteins conserved in all *Burkholderia* genomes was identified.
- We obtained a valuable platform for future experimental tests aimed to identify new molecular targets to be used in antimicrobial therapy against *Burkholderia* species.
- We refined the annotation of RND-like sequences in these genomes.

References

Papers of special note have been highlighted as:
▪ of interest
▪▪ of considerable interest

1. Saier MH Jr, Tam R, Reizer A, Reizer J. Two novel families of bacterial membrane proteins concerned with nodulation, cell division and transport. *Mol. Microbiol.* 11(5), 841–847 (1994).
2. Tseng TT, Gratwick KS, Kollman J *et al.* The RND permease superfamily: an ancient, ubiquitous and diverse family that includes human disease and development proteins. *J. Mol. Microbiol. Biotechnol.* 1(1), 107–125 (1999).

▪▪ **Complete description of the resistance–nodulation–cell division (RND) superfamily and of its various subfamilies.**

3. Saier MH Jr, Paulsen IT. Phylogeny of multidrug transporters. *Semin. Cell Dev. Biol.* 12(3), 205–213 (2001).

▪▪ **Discusses the phylogeny of the RND superfamily.**

4. Fani R, Fondi M. Origin and evolution of metabolic pathways. *Phys. Life Rev.* 6(1), 23–52 (2009).
5. Goel AK, Rajagopal L, Nagesh N, Sonti RV. Genetic locus encoding functions involved in biosynthesis and outer membrane localization of xanthomonadin in *Xanthomonas oryzae* pv. *oryzae*. *J. Bacteriol.* 184(13), 3539–3548 (2002).
6. Poole K, Krebes K, McNally C, Neshat S. Multiple antibiotic resistance in *Pseudomonas aeruginosa*: evidence for involvement of an efflux operon. *J. Bacteriol.* 175(22), 7363–7372 (1993).
7. Ma D, Cook DN, Alberti M, Pon NG, Nikaido H, Hearst JE. Molecular cloning and characterization of *acrA* and *acrE* genes of *Escherichia coli*. *J. Bacteriol.* 175(19), 6299–6313 (1993).
8. Aires JR, Kohler T, Nikaido H, Plesiat P. Involvement of an active efflux system in the natural resistance of *Pseudomonas aeruginosa* to aminoglycosides. *Antimicrob. Agents Chemother.* 43(11), 2624–2628 (1999).
9. Poole K. Efflux pumps as antimicrobial resistance mechanisms. *Ann. Med.* 39(3), 162–176 (2007).
10. Nikaido H, Takatsuka Y. Mechanisms of RND multidrug efflux pumps. *Biochim. Biophys. Acta* 1794(5), 769–781 (2009).
11. Nikaido H. Structure and mechanism of RND-type multidrug efflux pumps. *Adv. Enzymol. Relat. Areas Mol. Biol.* 77, 1–60 (2011).
12. Li XZ, Nikaido H. Efflux-mediated drug resistance in bacteria. *Drugs* 64(2), 159–204 (2004).
13. Li XZ, Nikaido H. Efflux-mediated drug resistance in bacteria: an update. *Drugs* 69(12), 1555–1623 (2009).
14. Murakami S, Nakashima R, Yamashita E, Yamaguchi A. Crystal structure of bacterial multidrug efflux transporter AcrB. *Nature* 419(6907), 587–593 (2002).
15. Sennhauser G, Bukowska MA, Briand C, Grutter MG. Crystal structure of the multidrug exporter MexB from *Pseudomonas aeruginosa*. *J. Mol. Biol.* 389(1), 134–145 (2009).
16. Akama H, Matsuura T, Kashiwagi S *et al.* Crystal structure of the membrane fusion protein, MexA, of the multidrug transporter in *Pseudomonas aeruginosa*. *J. Biol. Chem.* 279(25), 25939–25942 (2004).
17. Higgins MK, Bokma E, Koronakis E, Hughes C, Koronakis V. Structure of the periplasmic component of a bacterial drug efflux pump. *Proc. Natl Acad. Sci. USA* 101(27), 9994–9999 (2004).
18. Mikolosko J, Bobyk K, Zgurskaya HI, Ghosh P. Conformational flexibility in the multidrug efflux system protein AcrA. *Structure* 14(3), 577–587 (2006).
19. Koronakis V, Sharff A, Koronakis E, Luisi B, Hughes C. Crystal structure of the bacterial membrane protein TolC central to multidrug efflux and protein export. *Nature* 405(6789), 914–919 (2000).
20. Akama H, Kanemaki M, Yoshimura M *et al.* Crystal structure of the drug discharge outer membrane protein, OprM, of *Pseudomonas aeruginosa*: dual modes of membrane anchoring and occluded cavity end. *J. Biol. Chem.* 279(51), 52816–52819 (2004).
21. Su CC, Yang F, Long F *et al.* Crystal structure of the membrane fusion protein CusB from *Escherichia coli*. *J. Mol. Biol.* 393(2), 342–355 (2009).
22. Long F, Su CC, Zimmermann MT *et al.* Crystal structures of the CusA efflux pump suggest methionine-mediated metal transport. *Nature* 467(7314), 484–488 (2010).
23. Su CC, Long F, Zimmermann MT, Rajashankar KR, Jernigan RL, Yu EW. Crystal structure of the CusBA heavy-metal efflux complex of *Escherichia coli*. *Nature* 470(7335), 558–562 (2011).
24. Kulathila R, Indic M, van den Berg B. Crystal structure of *Escherichia coli* CusC, the outer membrane component of a heavy metal efflux pump. *PLoS ONE* 6(1), e15610 (2011).
25. Barnett MJ, Fisher RF, Jones T *et al.* Nucleotide sequence and predicted functions of the entire *Sinorhizobium meliloti* pSymA megaplasmid. *Proc. Natl Acad. Sci. USA* 98(17), 9883–9888 (2001).
26. Pinto FG, Chueire LM, Vasconcelos AT *et al.* Novel genes related to nodulation, secretion systems, and surface structures revealed by a genome draft of *Rhizobium tropici* strain PRF 81. *Funct. Integr. Genomics* 9(2), 263–270 (2009).
27. Eichler J. Evolution of the prokaryotic protein translocation complex: a comparison of archaeal and bacterial versions of SecDF. *Mol. Phylogenet. Evol.* 27(3), 504–509 (2003).
28. Hand NJ, Klein R, Laskewitz A, Pohlschroder M. Archaeal and bacterial SecD and SecF homologs exhibit striking structural and functional conservation. *J. Bacteriol.* 188(4), 1251–1259 (2006).
29. Pogliano KJ, Beckwith J. Genetic and molecular characterization of the *Escherichia coli secD* operon and its products. *J. Bacteriol.* 176(3), 804–814 (1994).
30. du Plessis DJ, Nouwen N, Driessen AJ. The Sec translocase. *Biochim. Biophys. Acta* 1808(3), 851–865 (2011).
31. Tsukazaki T, Mori H, Echizen Y *et al.* Structure and function of a membrane component SecDF that enhances protein export. *Nature* 474(7350), 235–238 (2011).
32. Quiblier C, Zinkernagel AS, Schuepbach RA, Berger-Bächi B, Senn MM. Contribution of SecDF to *Staphylococcus aureus* resistance and expression of virulence factors. *BMC Microbiol.* 11, 72 (2011).
33. Domenech P, Reed MB, Barry CE 3rd. Contribution of the *Mycobacterium tuberculosis* MmpL protein family to virulence and drug resistance. *Infect. Immun.* 73(6), 3492–3501 (2005).
34. La Rosa V, Poce G, Canseco JO *et al.* MmpL3 is the cellular target of the antitubercular pyrrole derivative BM212. *Antimicrob. Agents Chemother.* 56(1), 324–331 (2012).
35. Hausmann G, von Mering C, Basler K. The hedgehog signaling pathway: where did it come from? *PLoS Biol.* 7(6), e1000146 (2009).
36. Kuwabara PE, Labouesse M. The sterol-sensing domain: multiple families, a unique role? *Trends Genet.* 18(4), 193–201 (2002).
37. Schmerk CL, Bernards MA, Valvano MA. Hopanoid production is required for low-pH tolerance, antimicrobial resistance, and motility in *Burkholderia cenocepacia*. *J. Bacteriol.* 193(23), 6712–6723 (2011).
38. Doughty DM, Coleman ML, Hunter RC, Sessions AL, Summons RE, Newman DK. The RND-family transporter, HpnN, is required for hopanoid localization to the outer membrane of *Rhodopseudomonas*

palustris TIE-1. *Proc. Natl Acad. Sci. USA* 108(45), e1045–e1051 (2011).

39. Malott RJ, Steen-Kinnaird BR, Lee TD, Speert DP. Identification of hopanoid biosynthesis genes involved in polymyxin resistance in *Burkholderia multivorans*. *Antimicrob. Agents Chemother.* 56(1), 464–471 (2012).
40. Compant S, Nowak J, Coenye T, Clément C, Ait Barka E. Diversity and occurrence of *Burkholderia* spp. in the natural environment. *FEMS Microbiol. Rev.* 32(4), 607–626 (2008).

▪ **Description of the *Burkholderia* genus.**

41. Coenye T, Vandamme P. Diversity and significance of *Burkholderia* species occupying diverse ecological niches. *Environ. Microbiol.* 5(9), 719–729 (2003).

▪ **Description of the *Burkholderia* genus.**

42. Ormeño-Orrillo E, Rogel MA, Chueire LM, Tiedje JM, Martínez-Romero E, Hungria M. Genome sequences of *Burkholderia* sp. strains CCGE1002 and H160, isolated from legume nodules in Mexico and Brazil. *J. Bacteriol.* 194(24), 6927 (2012).
43. Lackner G, Moebius N, Partida-Martinez L, Hertweck C. Complete genome sequence of *Burkholderia rhizoxinica*, an endosymbiont of *Rhizopus microsporus*. *J. Bacteriol.* 193(3), 783–784 (2011).
44. Vanlaere E, Lipuma JJ, Baldwin A *et al.* *Burkholderia latens* sp. nov., *Burkholderia diffusa* sp. nov., *Burkholderia arboris* sp. nov., *Burkholderia seminalis* sp. nov. and *Burkholderia metallica* sp. nov., novel species within the *Burkholderia cepacia* complex. *Int. J. Syst. Evol. Microbiol.* 58(Pt 7), 1580–1590 (2008).
45. Vanlaere E, Baldwin A, Gevers D *et al.* Taxon K, a complex within the *Burkholderia cepacia* complex, comprises at least two novel species, *Burkholderia contaminans* sp. nov. and *Burkholderia lata* sp. nov. *Int. J. Syst. Evol. Microbiol.* 59(Pt 1), 102–111 (2009).
46. Govan JR, Brown AR, Jones AM. Evolving epidemiology of *Pseudomonas aeruginosa* and the *Burkholderia cepacia* complex in cystic fibrosis lung infection. *Future Microbiol.* 2(2), 153–164 (2007).
47. Bazzini S, Udine C, Riccardi G. Molecular approaches to pathogenesis study of *Burkholderia cenocepacia*, an important cystic fibrosis opportunistic bacterium. *Appl. Microbiol. Biotechnol.* 92(5), 887–895 (2011).
48. Drevinek P, Mahenthiralingam E. *Burkholderia cenocepacia* in cystic fibrosis: epidemiology and molecular mechanisms of virulence. *Clin. Microbiol. Infect.* 16(7), 821–830 (2010).
49. Bazzini S, Udine C, Sass A *et al.* Deciphering the role of RND efflux transporters in *Burkholderia cenocepacia*. *PLoS ONE* 6(4), e18902 (2011).
50. Guglierame P, Pasca MR, De Rossi E *et al.* Efflux pump genes of the resistance–nodulation–division family in *Burkholderia cenocepacia* genome. *BMC Microbiol.* 6, 66 (2006).

▪▪ **First analysis of RND-coding genes in *Burkholderia cenocepacia* J2315.**

51. Buroni S, Pasca MR, Flannagan RS *et al.* Assessment of three resistance–nodulation–cell division drug efflux transporters of *Burkholderia cenocepacia* in intrinsic antibiotic resistance. *BMC Microbiol.* 9, 200 (2009).
52. Nair BM, Cheung KJ Jr, Griffith A, Burns JL. Salicylate induces an antibiotic efflux pump in *Burkholderia cepacia* complex genomovar III (*B. cenocepacia*). *J. Clin. Invest.* 113(3), 464–473 (2004).
53. Kumar A, Mayo M, Trunck LA, Cheng AC, Currie BJ, Schweizer HP. Expression of resistance–nodulation–cell-division efflux pumps in commonly used *Burkholderia pseudomallei* strains and clinical isolates from northern Australia. *Trans. R. Soc. Trop. Med. Hyg.* 102(Suppl. 1), S145–S151 (2008).
54. Moore RA, DeShazer D, Reckseidler S, Weissman A, Woods DE. Efflux-mediated aminoglycoside and macrolide resistance in *Burkholderia pseudomallei*. *Antimicrob. Agents Chemother.* 43(3), 465–470 (1999).
55. Chan YY, Tan TM, Ong YM, Chua KL. BpeAB–OprB, a multidrug efflux pump in *Burkholderia pseudomallei*. *Antimicrob. Agents Chemother.* 48(4), 1128–1135 (2004).
56. Perrin E, Fondi M, Papaleo MC *et al.* Exploring the HME and HAE1 efflux systems in the genus *Burkholderia*. *BMC Evol. Biol.* 10, 164 (2010).

▪▪ **Analysis of two RND families in the *Burkholderia* genus.**

57. Altschul SF, Madden TL, Schaffer AA *et al.* Gapped BLAST and PSI-BLAST: a new generation of protein database search programs. *Nucleic Acids Res.* 25(17), 3389–3402 (1997).
58. Saier MH Jr, Tran CV, Barabote RD. TCDB: the transporter classification database for membrane transport protein analyses and information. *Nucleic Acids Res.* 34(Database issue), D181–D186 (2006).
59. Saier Jr MH, Yen MR, Noto K, Tamang DG, Elkan C. The Transporter Classification Database: recent advances. *Nucleic Acids Res.* 37(Database issue), D274–D278 (2009).
60. Edgar RC. MUSCLE: multiple sequence alignment with high accuracy and high throughput. *Nucleic Acids Res.* 32(5), 1792–1797 (2004).
61. Katoh K, Misawa K, Kuma K, Miyata T. MAFFT: a novel method for rapid multiple sequence alignment based on fast Fourier transform. *Nucleic Acids Res.* 30(14), 3059–3066 (2002).
62. Tamura K, Peterson D, Peterson N, Stecher G, Nei M, Kumar S. MEGA5: molecular evolutionary genetics analysis using maximum likelihood, evolutionary distance, and maximum parsimony methods. *Mol. Biol. Evol.* 28(10), 2731–2739 (2011).
63. Gasteiger E, Hoogland C, Gattiker A *et al.* Protein identification and analysis tools on the ExPASy server. In: *The Proteomics Protocols Handbook*. John M Walker (Ed.). Humana Press, NY, USA, 571–607 (2005).
64. Kyte J, Doolittle RF. A simple method for displaying the hydropathic character of a protein. *J. Mol. Biol.* 157(1), 105–132 (1982).
65. Zhai Y, Saier MH Jr. A web-based program for the prediction of average hydropathy, average amphipathicity and average similarity of multiply aligned homologous proteins. *J. Mol. Microbiol. Biotechnol.* 3(2), 285–286 (2001).
66. Sonnhammer EL, von Heijne G, Krogh A. A hidden Markov model for predicting transmembrane helices in protein sequences. *Proc. Int. Conf. Intell. Syst. Mol. Biol.* 6, 175–182 (1998).
67. Krogh A, Larsson B, von Heijne G, Sonnhammer EL. Predicting transmembrane protein topology with a hidden Markov model: application to complete genomes. *J. Mol. Biol.* 305(3), 567–580 (2001).
68. Marchler-Bauer A, Lu S, Anderson JB *et al.* CDD: a conserved domain database for the functional annotation of proteins. *Nucleic Acids Res.* 39(Database issue), D225–D229 (2011).
69. Marchler-Bauer A, Bryant SH. CD-Search: protein domain annotations on the fly. *Nucleic Acids Res.* 32(Web Server issue), W327–W331 (2004).
70. Hunter S, Jones P, Mitchell A *et al.* InterPro in 2011: new developments in the family and domain prediction database. *Nucleic Acids Res.* 40(Database issue), D306–D312 (2011).
71. Kumar A, Chua KL, Schweizer HP. Method for regulated expression of single-copy efflux pump genes in a surrogate *Pseudomonas aeruginosa* strain: identification of the BpeEF–OprC chloramphenicol and trimethoprim efflux pump of *Burkholderia pseudomallei* 1026b. *Antimicrob. Agents Chemother.* 50(10), 3460–3463 (2006).
72. Eda S, Yoneyama H, Nakae T. Function of the MexB efflux-transporter divided into two

halves. *Biochemistry* 42(23), 7238–7244 (2003).

73. Elkins CA, Nikaido H. Substrate specificity of the RND-type multidrug efflux pumps AcrB and AcrD of *Escherichia coli* is determined predominantly by two large periplasmic loops. *J. Bacteriol.* 184(23), 6490–6498 (2002).
74. Franke S, Grass G, Rensing C, Nies DH. Molecular analysis of the copper-transporting efflux system CusCFBA of *Escherichia coli*. *J. Bacteriol.* 185(13), 3804–3812 (2003).
75. Mao W, Warren MS, Black DS *et al.* On the mechanism of substrate specificity by resistance nodulation division (RND)-type multidrug resistance pumps: the large periplasmic loops of MexD from *Pseudomonas aeruginosa* are involved in substrate recognition. *Mol. Microbiol.* 46(3), 889–901 (2002).
76. Tikhonova EB, Wang Q, Zgurskaya HI. Chimeric analysis of the multicomponent multidrug efflux transporters from Gram-negative bacteria. *J. Bacteriol.* 184(23), 6499–6507 (2002).
77. Middlemiss JK, Poole K. Differential impact of MexB mutations on substrate selectivity of the MexAB–OprM multidrug efflux pump of *Pseudomonas aeruginosa*. *J. Bacteriol.* 186(5), 1258–1269 (2004).
78. Yen MR, Chen JS, Marquez JL, Sun EI, Saier MH. Multidrug resistance: phylogenetic characterization of superfamilies of secondary carriers that include drug exporters. *Methods Mol. Biol.* 637, 47–64 (2010).
79. Baldwin A, Mahenthiralingam E, Thickett KM *et al.* Multilocus sequence typing scheme that provides both species and strain differentiation for the *Burkholderia cepacia* complex. *J. Clin. Microbiol.* 43(9), 4665–4673 (2005).
80. Vandamme P, Dawyndt P. Classification and identification of the *Burkholderia cepacia* complex: past, present and future. *Syst. Appl. Microbiol.* 34(2), 87–95 (2011).

Websites

101. GenBank database. www.ncbi.nlm.nih.gov
102. Transport Classification Database. www.tcdb.org
103. Protein section of the NCBI database. www.ncbi.nlm.nih.gov/protein
104. ExPASy website. http://expasy.org
105. Conserved Domain database. www.ncbi.nlm.nih.gov/Structure/cdd/cdd.shtml
106. InterProScan sequence search. www.ebi.ac.uk/Tools/pfa/iprscan
107. Genome section of the NCBI database. www.ncbi.nlm.nih.gov/genome

OPEN ACCESS Freely available online

PLoS one

Deciphering the Role of RND Efflux Transporters in *Burkholderia cenocepacia*

Silvia Bazzini[1☯], Claudia Udine[1☯], Andrea Sass[2☯], Maria Rosalia Pasca[1], Francesca Longo[3], Giovanni Emiliani[4], Marco Fondi[5], Elena Perrin[5], Francesca Decorosi[6], Carlo Viti[6], Luciana Giovannetti[6], Livia Leoni[3], Renato Fani[5], Giovanna Riccardi[1], Eshwar Mahenthiralingam[2], Silvia Buroni[1]*

1 Dipartimento di Genetica e Microbiologia, Università degli Studi di Pavia, Pavia, Italy, **2** Cardiff School of Biosciences, Cardiff University, Cardiff, Wales, United Kingdom, **3** Dipartimento di Biologia, Università Roma Tre, Roma, Italy, **4** Trees and Timber Institute – National Research Council, San Michele all'Adige, Italy, **5** Department of Evolutionary Biology, University of Florence, Firenze, Italy, **6** Dipartimento di Biotecnologie Agrarie, Università degli Studi di Firenze, Firenze, Italy

Abstract

Burkholderia cenocepacia J2315 is representative of a highly problematic group of cystic fibrosis (CF) pathogens. Eradication of *B. cenocepacia* is very difficult with the antimicrobial therapy being ineffective due to its high resistance to clinically relevant antimicrobial agents and disinfectants. RND (Resistance-Nodulation-Cell Division) efflux pumps are known to be among the mediators of multidrug resistance in Gram-negative bacteria. Since the significance of the 16 RND efflux systems present in *B. cenocepacia* (named RND-1 to -16) has been only partially determined, the aim of this work was to analyze mutants of *B. cenocepacia* strain J2315 impaired in RND-4 and RND-9 efflux systems, and assess their role in the efflux of toxic compounds. The transcriptomes of mutants deleted individually in RND-4 and RND-9 (named D4 and D9), and a double-mutant in both efflux pumps (named D4-D9), were compared to that of the wild-type *B. cenocepacia* using microarray analysis. Microarray data were confirmed by qRT-PCR, phenotypic experiments, and by Phenotype MicroArray analysis. The data revealed that RND-4 made a significant contribution to the antibiotic resistance of *B. cenocepacia*, whereas RND-9 was only marginally involved in this process. Moreover, the double mutant D4-D9 showed a phenotype and an expression profile similar to D4. The microarray data showed that motility and chemotaxis-related genes appeared to be up-regulated in both D4 and D4–D9 strains. In contrast, these gene sets were down-regulated or expressed at levels similar to J2315 in the D9 mutant. Biofilm production was enhanced in all mutants. Overall, these results indicate that in *B. cenocepacia* RND pumps play a wider role than just in drug resistance, influencing additional phenotypic traits important for pathogenesis.

Citation: Bazzini S, Udine C, Sass A, Pasca MR, Longo F, et al. (2011) Deciphering the Role of RND Efflux Transporters in *Burkholderia cenocepacia*. PLoS ONE 6(4): e18902. doi:10.1371/journal.pone.0018902

Editor: Mark Alexander Webber, University of Birmingham, United Kingdom

Received December 21, 2010; **Accepted** March 11, 2011; **Published** April 19, 2011

Funding: This research was supported by grants from the Italian Cystic Fibrosis Research Foundation (FFC) to G.R. (Project FFC#15/2009, adopted by Pastificio Rana S.p.A.) and to L.L. (Project FFC#14/2010). A.S. and E.M. acknowledge support for the microarray analysis by the US Cystic Fibrosis Therapeutics program (grant number MAHENT06V0). The funders had no role in study design, data collection and analysis, decision to publish, or preparation of the manuscript.

Competing Interests: The authors have declared that no competing interests exist.

* E-mail: silvia.buroni@unipv.it

☯ These authors equally contributed to the work.

Introduction

The *Burkholderia cepacia* complex (Bcc) constitutes a group of phenotypically similar non-fermenting, aerobic, Gram-negative rods that infect 2 to 8% of patients with cystic fibrosis (CF) [1]. Bcc comprises at least 17 different closely related species whose correct identification is particularly important in clinical microbiology as these bacteria are opportunistic pathogens that can cause severe lung infections in immuno-compromised as well as in CF patients [1].

In CF patients, antibiotics are used to clear early infection, treat acute exacerbations of chronic infection and reduce their relapse frequency. These treatments have had a major impact on the quality and survival of CF patients [2]. Despite the heavy use of antibiotics in CF, over the last decades, *B. cenocepacia* has emerged as an important respiratory pathogen in the CF community. Pulmonary colonization/infection by this bacterium may persist for months or even years but a minority of patients exhibits a rapid clinical deterioration associated with severe respiratory inflammation, epithelial necrosis and invasive disease, a condition known as cepacia syndrome [3,4].

The *B. cenocepacia* epidemic ET12 lineage that originated in Canada and spread to Europe has been one of the most prevalent Bcc genotypes isolated from CF patients, with strain J2315 being studied in depth as model isolate [5]. The 8.06-Mb genome of this highly transmissible pathogen, consisting of three circular chromosomes and a plasmid, encodes a broad array of functions typical of metabolically versatile genus *Burkholderia*, as well as several virulence and drug resistance functions [5]. Antimicrobial therapy for Bcc is often ineffective as members of the *B. cepacia* complex are highly resistant to most clinically relevant antimicrobial agents and disinfectants [6]. Multi-drug resistance (MDR) in CF isolates is defined as resistance to all of the agents belonging to at least two of three classes of antibiotics, such as quinolones, aminoglycosides, and β-lactam agents, including monobactams and carbapenems [7].

Particularly interesting among mediators of MDR in Gram-negative bacteria are transporters belonging to the RND

(Resistance-Nodulation-Cell Division) family, whose members catalyze the active efflux of many antibiotics and chemotherapeutic agents [8]. RND transporters are protein complexes that span both the cytoplasmic and outer membrane. The complex comprises a cytoplasmic membrane transporter protein, a periplasmic-exposed membrane adaptor protein, and an outer-membrane channel protein. The *Escherichia coli* AcrAB-TolC and the *Pseudomonas aeruginosa* MexAB-OprM complexes are well characterized; besides, the resolution of the three-dimensional structures of various components supported the model according to which these efflux systems form a channel for the extrusion of substrates/drugs from within the cell envelope back into the external environment [9–13]. There are also a number of studies suggesting that RND efflux systems play important roles in bacterial pathogenesis, participating in colonization and persistence of bacteria in the host, as well as in metal ion homeostasis [14,15].

The significance of RND efflux systems in *B. cenocepacia* has been only partially determined. We have previously identified 14 genes encoding putative RND efflux pumps in the genome of *B. cenocepacia* J2315 [16]. After the completion of the whole genome sequence [5], two additional genes encoding RND pumps were discovered and, very recently, a complete description of the distribution of RND proteins within *Burkholderia* genus was obtained [17]. We named the operons encoding the *B. cenocepacia* RND efflux pumps RND-1 to RND-16 [18]. Most of these operons comprise the membrane fusion protein, the RND pump, and the outer membrane protein encoding genes.

Systematic measures of the role that RND efflux systems play in *Burkholderia* can be obtained by deleting single or multiple *rnd* operons and examining the genotype and phenotype of the resulting mutants. However, *B. cenocepacia* strain J2315 is difficult to manipulate genetically, in part due to its high level of antibiotic resistance, which precludes the use of the most common selectable markers for gene exchange. For this reason, also in our previous work, we adopted a recently developed mutagenesis strategy [19] to obtain *rnd* knockout mutants of *B. cenocepacia* J2315 [18]. The mutagenesis strategy we employed has the advantage of generating markerless deletions, making it possible to repeatedly use the same antibiotic resistance cassette for engineering subsequent gene deletions [19]. We successfully deleted three of these operons in *B. cenocepacia* strain J2315, encoding the putative RND-1, RND-3, and RND-4 transporters (namely BCAS0591-BCAS0593, BCAL1674-BCAL1676, and BCAL2822-BCAL2820 genes) and the corresponding inactivated strains were named D1, D3, and D4. The mutant phenotypes demonstrated that RND-3 and RND-4 contributed significantly to the antibiotic resistance of *B. cenocepacia* [18].

The availability of *rnd* knockout mutants in *B. cenocepacia* J2315 is a good starting point to further investigate the role of these efflux systems not only in antibiotic resistance but also in other metabolic pathways, including those relevant for pathogenesis. In fact, multidrug transporter genes are frequently subjected to both local and global regulation and are taking part in complex transcriptional networks, which may be elucidated by transcriptome analysis. Hence, the aim of this work was to analyze mutants of *B. cenocepacia* J2315 impaired in *rnd* genes to assess their role in the efflux of toxic compounds and physiology of *B. cenocepacia* by comparing the transcriptome of mutants with that of the wild-type strain using microarray analysis. We focused our attention on the previously characterized D4 strain, as it showed an interesting phenotype regarding drug resistance [18], and a novel mutant D9 [20], which was impaired in RND-9 operon (encoded by BCAM1945-1947 genes). We chose D9 since it has been recently shown by a combination of *in silico* analyses that BCAM1946 (RND-9) belongs to the HAE-1 family comprising proteins responsible for the extrusion of antibiotics [17], and thus might be able to pump out toxic compounds. However, the deep phylogenetic analysis performed by Perrin *et al.* [17] showed also that the BCAM1946 protein sequence joined the same cluster as BCAL2821 (RND-4), even if they belong to different and distant branches, and has a narrow phylogenetic distribution, in that its orthologs are present only in a few Bcc species. This finding suggests that RND-4 and RND-9 might be involved in different physiologic processes. Further, this operon was chosen as BCAM1947 gene was found to be over-expressed in the *sputum* of CF patients [21] and because the whole operon shares amino acid identity with the more known MexEF-OprN efflux system of *P. aeruginosa* [22,23]. In fact, the product of BCAM1945 possesses a 38% amino acid sequence identity with OprN from *P. aeruginosa*, while BCAM1946 has a 56% of identity with MexF and BCAM1947 a 46% with MexE.

Hence, in this work we tried to shed some light on the role that RND-4 and RND-9 might have in cell physiology and in particular in the efflux of toxic compounds by analysing the transcriptome of three mutants: D4, which was previously described [18], D9 and D4–D9, single and double mutants respectively. Microarray data were confirmed by qRT-PCR and phenotypic experiments, as well as by Phenotype MicroArray analysis.

Materials and Methods

Bacterial strains and growth conditions

Bacterial strains and plasmids used in this study are listed in Table 1. Bacteria were grown in Luria-Bertani (LB) broth (Difco), with shaking at 200 rpm, or on LB agar, at 37°C. The construction of mutants D4, D9 and D4–D9 has been described in other papers [18,20].

MIC determination

Determination of MIC (Minimal Inhibitory Concentration) for *B. cenocepacia* J2315 and the deleted mutants D9 and D4–D9 was performed by streaking 1×10^4 cells onto LB agar containing 2-fold dilutions of different drugs. The MIC was defined as the lowest drug concentration that prevented visible growth. The following compounds were tested to determine the resistance profile: aztreonam, ethidium bromide, chloramphenicol, gentamicin, tobramicin, nalidixic acid, ciprofloxacin, levofloxacin, norfloxacin, sparfloxacin, ampicillin, ceftazidime, erythromycin, meropenem, piperacillin, kanamycin and trimethoprim. Plates were incubated at 37°C for 3 days and growth was visually evaluated. The results represent the average of three independent replicates. The significance of MIC differences between the strains was assessed using the Wilcoxon rank-sum test.

RNA purification and preparation for microarrays

For the microarray and qRT-PCR experiments, wild-type and mutant *B. cenocepacia* J2315 cells were harvested by centrifugation and transferred into sterile tubes. Total RNA was purified using the RiboPure Bacteria Kit (Ambion) according to the manufacturer's instructions. 1×10^9 cells were used for three biological replicates of each strain (J2315, D4, D9 and D4–D9).

A 1 hour incubation of each sample with DNase I (Ambion) was used, following the manufacturer's instructions. After extraction, the RNA was concentrated using the LiCl method [24]. RNA quality and concentration were assessed using the Agilent 2100 Bioanalyzer (Agilent) and agarose gel electrophoresis. All RNA

Table 1. Strains and plasmids used in this work.

Strain or plasmid	Relevant characteristics	Source and/or reference
***B. cenocepacia* strains**		
J2315	CF clinical isolate	G. Manno
D4	J2315 ΔBCAL2820-BCAL2822	[18]
D9	J2315 ΔBCAM1945-BCAM1948	[20]
D4–D9	J2315 ΔBCAM1945-BCAM1948 ΔBCAL2820-BCAL2822	[20]
***E. coli* strains**		
DH5α	F^- Φ80d*lacZ*ΔM15 Δ(*lacZYA-argF*)*U169 endA1 recA1 hsdR17*(r_K^- m_K^+) *supE44 thi-1* Δ*gyrA96 relA1*	Laboratory stock
SY327	*araD* Δ(*lac pro*) *argE*(Am) *recA56 nalA* λ. *pir*, Rif^r	M.A. Valvano
Plasmids		
pGEM-T Easy	Vector for PCR cloning, Amp^r	Promega
pGPISce-I	ori_{R6K}, ΩTp^r, *mob*$^+$, containing the ISce-I restriction site, Tp^r	M.A. Valvano
pRK2013	ori_{ColE1}, RK2 derivative, Kan^r, *mob*$^+$, *tra*$^+$, Kan^r	M.A. Valvano
pDAISce-I	pDA12 encoding the ISce-I homing endonuclease, Tet^r	M.A. Valvano

Amp^r, ampicillin resistance; Kan^r, kanamycin resistance; Rif^r, rifampin resistance; Tet^r, tetracycline resistance; Tp^r, trimethoprim resistance.
doi:10.1371/journal.pone.0018902.t001

samples fulfilled the requirements for microarray experiments. 10 µg of total RNA were used for labeling reactions. cDNA generation and labeling was performed using the CyScribe Post-Labeling kit (GE Healthcare) according to the manufacturer's instructions and including spike-in controls for quality control (Agilent). cDNA was purified by ethanol precipitation and the purification of the labeled cDNA was performed using the CyScribe GFX purification kit. For the elution, water was used instead of the buffer provided by the kit. The quantification of the amount of generated cDNA and of Cy dye was performed with a NanoDrop spectrophotometer.

Microarray hybridization and analysis

The microarrays used were 4×44 K 60-mer arrays that contain spots corresponding to all coding regions of *B. cenocepacia* J2315 genome (a total 7251 probes including duplicate probes for several genes) and also probes corresponding to selected intergenic regions (1489). Hybridization and washing were performed following the "Two-colour microarray based gene expression analysis" protocol from Agilent, with the following exceptions: fragmentation buffer was not used, 1 µl of a mixture of labeled oligonucleotides was added, and the mixture of cDNA was incubated at 98°C for 3 minutes for denaturing. The hybridization buffer was from the Gene Expression Hybridization kit. The microarrays were scanned using a microarray scanner (G2565 BA, Agilent) and the Scan Control software version A.7.0.3. Feb 2007 (Agilent). The scan region was adjusted to 61×21.6 mm and the scanning resolution was set to 5 µm. The Extended Dynamic Range function was switched on with 100% and 10% PMT gain settings. The images were analysed with the Feature Extraction software version 9.5.1. Feb 2007 (Agilent) and the FE protocol used was GE2_v5_95_Feb07 with default settings. GeneSpring was used to analyze gene expression data. The data were filtered based on expression level changes of greater than 1.5-fold. Differentially expressed genes were filtered on t-test p-value with a threshold of 0.05 (parametric test which does not assume the variances as equal: Welch's t-test) without multiple testing correction.

The software Blast2GO (version 2.3.4) [25] was used, with default parameters, to obtain the functional annotation of the differentially expressed transcripts as well as the related gene ontology (GO) terms. Blast2GO was also used for GO functional enrichment analysis of genes, by performing Fisher's exact test with robust false discovery rate (FDR) correction to obtain an adjusted p-value between certain test gene groups and the whole annotation.

Quantitative Real-Time PCR (qRT-PCR)

For each strain six unlinked genes were chosen for qRT-PCR based on their differential expression pattern and annotation. Three genes were chosen among the up-regulated ones and three among the down-regulated ones. cDNA was synthesized using the M-MLV Reverse Transcriptase (Promega) and using 2 µg of total RNA as starting material. cDNA was precipitated, resuspended in DEPC water and stored at −80°C. Primer sequences for quantitative PCR are listed in Table 2. qRT-PCR reactions were performed on a Rotor-Gene-6000 cycler (Corbett), using Quanti-Fast SYBR Green PCR Kit (QIAGEN) according to the manufacturer's protocol except that 10 µl were used as a final volume for each reaction. Cycling conditions were: 95°C for 5 min (1 cycle), 95°C for 10 sec followed by 60°C for 30 sec (35 cycles). A melting curve analysis was included at the end of each run. Each sample was spotted in triplicate and a reference gene as well as control samples without cDNA were included in each experiment. The BCAM0166 (*ndh*) gene showed a stable expression in the different strains and was used as reference gene. The comparative Ct-method was used to determine the fold difference in gene expression between the mutant strains and the wild-type.

The comparison of gene expression fold change, obtained both by microarray analysis and qRT-PCR, was assessed by Pearson correlation.

Swimming, biofilm and chemotaxis assays

For swimming assays, LB grown *B. cenocepacia* cultures ($A_{600\ nm} = 1.0$) were inoculated with a toothpick on 'swimming plates' (1 g/l tryptone, 0.5 g/l yeast extract, 5 g/l NaCl, 3 g/l agar noble) and incubated for 42 hours at 37°C. In this growth medium bacteria can swim through the soft agar and produce a halo. The diameter of the halo is a measure of the ability to swim.

Table 2. Primers used in this work.

Primer name	Primer sequence
Bcal0114F	5′-CGGATGCAGACCCAGAT-3′
Bcal0114R	5′-TGCAGGCTGTTCGTCAG-3′
Bcal0135F	5′-AACATGCCGAACCTCG-3′
Bcal0135R	5′-GCGATGATGTTCTCCTT-3′
Bcal0140F	5′-GTGCCTTACCAACTCT-3′
Bcal0140R	5′-CTGCTGCTGGCGAATG-3′
Bcal0178F	5′-TTGGGCGACTCAATGG-3′
Bcal0178R	5′-TTCGTGTATGGCGGAT-3′
Bcal0520F	5′-CCTGCTTCCATCGCTT-3′
Bcal0520R	5′-ACGCTCAACCCGCCCG-3′
Bcal0566F	5′-TCGTACACCAACAGCG-3′
Bcal0566R	5′-TGAGCCCCACCGTCGT-3′
Bcal0577F	5′-GCAGGTCAGCAGCAAC-3′
Bcal0577R	5′-CTGCGCGTAAGCCTTCT-3′
Bcal1828F	5′-GCATCAGGCGGCTTAC-3′
Bcal1828R	5′-CGCTTCGTCGGGAAAC-3′
Bcal3152F	5′-CTGCTGACGCTGTTGC-3′
Bcal3152R	5′-AACTCCAGCCCGCCGAC-3′
Bcam0726F	5′-GCAGCATGAACCACAC-3′
Bcam0726R	5′-CTGGCAAAGACGAACC-3′
Bcam1484F	5′-AGCATCCCGATCAGGT-3′
Bcam1484R	5′-GGCGAAGCGGAAGACG-3′
Bcam2616F	5′-CTGCACGACCTGCTGG-3′
Bcam2616R	5′-TGCCGGTCTGCTCCTG-3′
Bcam0695F	5′-CGGGGCGAGCGGGTTG-3′
Bcam0695R	5′-CCTCGGCGGCGTCGTG-3′
Bcam0727F	5′-AGGTCGGCGGGCAGGA-3′
Bcam0727R	5′-GCGGTACAGGTGTTCG-3′
ndhF	5′-GCGATCGGGCTGTACAAGTT-3′
ndhR	5′-AGTGGCTCAGCGACTGGAA-3′

doi:10.1371/journal.pone.0018902.t002

Crystal violet binding assay was carried out using 96-wells plates pre-treated with mucin as described by Rose *et al.* [26]. Bacterial cultures were grown in LB and diluted to $A_{600} = 0.01$; 150 µL of each strain was then placed into 96-well plates. The plates were incubated at 37°C statically for 72 hours. After incubation, the plates were washed three times with PBS to remove planktonic growth. The remaining biofilm was fixed with methanol for 15 min. Once methanol was removed and plates were dried, biofilms were stained with 1% Crystal Violet for 5 min. The stain was removed by washing with water and plates were dried. Biofilm thickness was measured by adding 33% glacial acetic acid and taking an OD reading at 600 nm using an automated plate reader [26].

The Congo red binding assay was carried out as previously described, with slight modifications [27]. Briefly, bacteria were grown on LB agar plates for 72 hours at 37°C. Colonies were scraped off, suspended in 9 g/l NaCl and normalized to a $A_{600\ nm} = 2.0$. Cells from 1 ml of bacterial suspension were harvested by centrifugation, suspended in 1 ml of Congo red buffer [0.002% (w/v) Congo red dye (Sigma-Aldrich), 9 g/l NaCl] and incubated at room temperature for 10 min. Samples were then centrifuged for 5 min at 6000 rpm and the optical density at 500 nm wavelength ($A_{500\ nm}$) of the supernatant was measured. The amount of Congo red dye not retained by the cells was estimated by measuring the absorbance at $A_{500\ nm}$ of the supernatants. $A_{500\ nm}$ levels are in inverse proportion to exopolysaccharide and fimbrial structures production. The Congo red binding of *B. cenocepacia* J2315 is defined as one hundred percent binding.

For all the above described assays the average of the results obtained from three independent experiments are reported with standard deviation. The statistical significance of the observed differences in mean invasion frequencies was determined by calculating the p-values using the two-tailed Student t test for unpaired data sets. p-values are reported in figure legends.

The *Burkholderia* chemotaxis assay was slightly modified from Leungsakul *et al.*, [28]. Cells in the exponential phase of growth or heat-killed cells (negative control) were washed and resuspended in drop assay medium (MSB containing 0.2% bacto-agar and 10 mM succinate as an energy source) and poured in Petri plates. 10 µl of 40% tryptone or 40 X LB or 20% yeast extract were poured at the centre of each plate. 10 µl of 20% casamino acids solution was used as a positive control. Heat-killed cells for negative controls were prepared by autoclaving at 121°C for 30 min (control for non-chemotactic aggregation). No-substrate negative controls were also used. The chemotactic response was assessed after 18 hours.

Phenotype MicroArray (PM) tests

The four *B. cenocepacia* strains J2315, D4, D9 and D4–D9 were tested on chemical sensitivity PM panels (PM11–PM20) (Biolog) for 960 different conditions including several concentrations of a wide variety of antibiotics, antimetabolites, heavy metals and other inhibitors. A tetrazolium dye is used as a reporter of active metabolism [29]. The reduction of the dye causes the formation of a purple colour that is recorded by a CCD camera every 15 min and provides quantitative and kinetic information about the response of cells in the tested conditions.

The wild-type strain and the three mutants were grown 36 hours at 37°C on BUG agar (Biolog). A cellular suspension in IF-0 (Biolog), whose density was adjusted to 80% transmittance by a Biolog turbidimeter, was prepared for each strain. The cellular suspension was diluted 13.64 times in IF-10 GN/GP (Biolog), dye G (Biolog) was added, according to the Biolog instructions, and used for plate inoculation. All PM plates were incubated at 37°C in an Omnilog reader (Biolog). Readings were recorded for 48 hours and data were analysed with Omilog-PM software (release OM_PM_109 M) (Biolog).

The data from the Omnilog-PM software were filtered, using the area of the kinetic curves as a parameter, then transferred to Excel spreadsheets (Microsoft Corporation) and processed with Bionumerics software (Applied Math) for principal-component analysis (PCA) in order to establish the correlations between the phenotype profiles of the strains.

The Omnilog-PM software also allowed the IC50 value to be determined for each chemical tested (four concentrations of each chemical were present in the plates from PM11 to PM20). IC50 is expressed in well units and should be defined as the well or fraction of a well at which a particular per-well parameter (*i.e.* the area of the curve) is at half of its maximal value over a concentration series. The half-maximal value most likely falls between the per-well parametric values of two consecutive wells, in which case, a fraction of a well is interpolated from the half-maximal value (Biolog, personal communication).

Microarray data accession numbers

The raw microarray data (J2315 and D4) can be found in ArrayExpress under the accession number E-MEXP-2999. The raw data (J2315, D9 and D4–D9) can be found in ArrayExpress under the accession number E-MEXP-2997.

Results

Resistance profile of *rnd* operon deleted mutants

In order to investigate the contribution of efflux pumps to intrinsic drug resistance of *B. cenocepacia* J2315, we recently deleted 3 operons encoding the putative RND transporters RND-1, RND-3, and RND-4 [18]. In this work we continued in the same direction and analyzed the effect of the deletion of operon encoding RND-9 efflux pump in the wild-type strain (D9 mutant), as well as in the D4 strain (the double D4-D9 mutant) [20]. RND-9, which is located on chromosome 2, comprises genes BCAM1945-1947. It is noteworthy that in the D9 and D4-D9 mutant strains the BCAM1948 gene, encoding a MerR transcriptional regulator and hypothesized to control the expression of RND-9 operon, was inactivated, too [20].

The strains D9 and D4-D9 were tested for their susceptibility to a number of drugs, in comparison to the wild-type strain *B. cenocepacia* J2315. Strain D9 showed a 2-fold decrease of the MIC value of aztreonam, ethidium bromide, tobramycin, levofloxacin, and sparfloxacin in respect to the wild-type strain (Table 3). The D4-D9 double mutant exhibited a 4 to 16-fold increase in drug susceptibility to several of the antimicrobials tested: in particular, it is more susceptible than the wild-type strain but comparable to the D4 mutant when exposed to aztreonam, chloramphenicol, ethidium bromide, gentamicin, tobramycin, and to different fluoroquinolones, such as nalidixic acid, ciprofloxacin, levofloxacin, norfloxacin, sparfloxacin. Furthermore, the MIC for nalidixic acid was 16-fold lower in D4–D9 than in J2315 and 4-fold lower than in D4 (Table 3). The MIC values of other drugs such as ampicillin, ceftazidime, meropenem, piperacillin, erythromycin, and kanamycin were not altered in the D9 and in the D4–D9 as compared to J2315 (data not shown).

The significance of MIC differences between the strains was assessed using the Wilcoxon rank-sum test and all the differences in antimicrobial susceptibility were statistically significant ($p<0.05$).

Table 3. Antimicrobial susceptibilities (μg/ml) of *B. cenocepacia* J2315, D9 and D4-D9 mutant strains.

Compound	Strain			
	J2315	D4	D9	D4–D9
Aztreonam	2000	250	1000	250
Ethidium bromide	2000	125	1000	125
Chloramphenicol	4	1	4	1
Gentamicin	2000	1000	2000	1000
Tobramycin	1000	250	500	250
Nalidixic acid	16	4	16	1
Ciprofloxacin	8	2	8	2
Levofloxacin	4	0.5	2	0.5
Norfloxacin	32	8	32	8
Sparfloxacin	8	1	4	1

doi:10.1371/journal.pone.0018902.t003

Transcriptome analysis

In order to derive more information about the biological role of RND transporters, transcriptome analysis was carried out by using *B. cenocepacia* J2315, D4, D9 and D4-D9 strains. After a global analysis of the microarray data obtained, different gene lists were generated: genes induced in each mutant *versus* wild-type J2315, down-regulated genes in each mutant strain *versus* J2315 and differentially expressed genes overlapping in different mutants. A complete list of the microarray data is reported in Table S1.

Overall, our analyses showed that 216 genes were differentially expressed in D4 mutant in respect to the wild-type strain (Table S1), corresponding to 3% of the total 7251 probes used in this work. Among them, 32 encoded hypothetical proteins with unknown function. 138 CDSs (64%) were up-regulated and 78 (36%) down-regulated (Table S1). 118 among the differentially expressed genes in D4 mutant were located on chromosome 1 (55%), 55 on chromosome 2 (25%), and 42 (20%) on chromosome 3. 60 intergenic regions appeared to be differentially expressed in D4 strain (39 up-regulated and 21 down-regulated, Table S1).

The D9 mutant showed 168 genes differentially expressed in respect to the wild-type strain (Table S1). Among them, 43 encoded proteins with unknown function and 1 was not annotated. 61 CDSs (36%) were up-regulated and 107 down-regulated (64%) (Table S1). 66 (40%) out of 168 differentially expressed genes were located on chromosome 1, 73 (43%) on chromosome 2 and 29 (17%) on chromosome 3. Moreover, also 26 intergenic regions resulted to be differentially expressed in this mutant (8 were up-regulated and 18 down-regulated, Table S1).

In the case of the D4–D9 strain, 550 differentially expressed genes (7.6% of the total probes) were detected. 257 of them (47% of the differentially expressed genes) resulted to be up-regulated, while 293 (53%) were down-regulated. 110 encoded proteins with unknown function and 1 was not annotated (Table S1). 259 out of 550 differentially expressed genes were located on chromosome 1 (47%), 221 (40%) on chromosome 2, 67 (12%) on chromosome 3, and 3 (less than 1%) on the plasmid. In the case of D4–D9 mutant, also 84 intergenic regions resulted to be differentially expressed (31 up-regulated and 53 down-regulated) respect to the wild-type strain.

A χ^2 analysis of the distribution of the differentially expressed genes on each chromosome was performed. In the case of D4 and D9 strains, the results indicate that there is a significant correlation between the number of differentially expressed genes and their location on each chromosome, *i.e.* the proportion of differentially expressed genes of each chromosome is correlating to the total number of genes on each chromosome. This was not observed with the D4-D9 double mutant.

Among the differentially expressed genes, it was possible to find some similarities shared by our efflux pump deleted strains (Figure 1). In particular, 33 genes resulted to be differentially expressed with respect to the J2315 strain in all the mutants described in this work (Table S1), with 24 of them being up-regulated in all mutants, and 9 down-regulated (Figure 1). 84 genes were differentially expressed in both D9 and D4–D9 mutants; interestingly, only BCAM1697 resulted to be up-regulated in D9 and down-regulated in the double mutant, while the expression profile of all the other genes was consistent in both strains, 63 being down-regulated and 21 up-regulated (Table S1, Figure 1). As regarding D4 and D4-D9 mutants, 123 genes resulted to be differentially expressed in both (44 down-regulated and 79 up-regulated, all consistent in both strains, Table S1). These concepts are clarified by the Venn diagram shown in Figure 1.

Major classes of *B. cenocepacia* genes with altered expression in the mutant strains in respect to the wild-type were identified (see

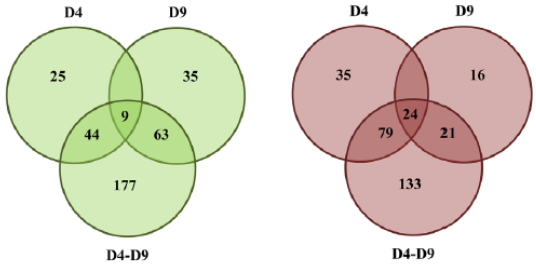

Figure 1. Differential gene regulation in the *B. cenocepacia* RND efflux mutants. The Venn diagram represents the differently expressed genes (down-regulated on the left, up-regulated on the right) in each mutant with respect to the wild-type strain.
doi:10.1371/journal.pone.0018902.g001

supplemental files: Table S1 and Figures S1, S2, S3, S4, S5, S6). Using a functional enrichment analysis of genes (see supplemental files: Tables S2, S3, S4, S5, S6, S7) it was possible to individuate statistically significant functional categories that are over- or under- represented in the differentially expressed gene-lists of the efflux pump(s)-deleted mutant strains described in this work in respect to the wild-type. The composition of these gene groups is discussed in more detail below.

Flagellum mediated motility

Like many other microorganisms, *B. cepacia* complex bacteria are motile and use complex protein structures called flagella. They possess one or longer polar flagella responsible for swimming motility. Many biological processes other than motility require the presence of these structures, for example the production of biofilms, adherence and invasion into host cells [30–32]. Flagella represent one of the virulence factors which contribute to the development of disease caused by these bacteria as shown by *in vivo* data [33]. They have been described as a major factor contributing to host inflammatory responses to bacteria due to the interaction of bacterial flagellin with the Toll-like receptor 5 (TLR5) [34–36].

The production and assembly of these multi-component structures involve more than 40 genes. In particular, members of the Bcc express one of two types of flagellin that can be distinguished by size (55 kDa for type I and 45 kDa for type II) and restriction fragment length polymorphism (RFLP) patterns of the *fliC* gene [37,38].

The results obtained from the comparison of the microarray analysis of *B. cenocepacia* J2315 with D4, D9 and D4–D9 mutants showed that a large proportion of the differentially expressed genes were involved in flagellum assembly and motility (Table S1, Figures S1, S4 and S5). In particular, D4 and D4-D9 mutants shared 26 up-regulated flagellum-related genes (Table 4). Among them we found: *fliC* (BCAL0114), encoding the major structural component of flagellin, and BCAL0521 encoding the flagellar protein FliJ; BCAL0140-BCAL0143, BCAL0523, BCAL0527, BCAL0561, and BCAL3501, which code for flagellar biosynthesis proteins and assembly; BCAL0113, BCAL0520, BCAL0567 and BCAL0577 encoding the hook-associated proteins. Moreover, some genes belonging to the flagellar regulon master regulator *flh* (BCAL0124 and BCAL0125) were also over-expressed in these mutants (Table 4). Lastly, some flagellar basal body Rod protein encoding genes (BCAL0565, BCAL0566, BCAL0568, BCAL0569, and BCAL3507) were up-regulated and shared by the two mutants, as like as P- and L-ring proteins encoding ones (BCAL0570 and BCAL0571) (Table 4).

In addition to the genes mentioned above, D4 mutant over-expressed 12 additional flagellum-associated genes, four of which coding for flagellar motor proteins (BCAL0524, BCAL3506, BCAM0777, and BCAM0778) and other two for flagellar basal body Rod protein (BCAL0564 and BCAM0987) (Table 4).

In contrast, the D9 mutant showed an enrichment of motility related genes in the down-regulated gene list (BCAL0125, BCAL0140, BCAL0142, BCAL0520, BCAL0522, BCAL0566, BCAL0567, BCAL0568, BCAL0570, BCAL0571) (Table 4; Figure S4).

Chemotaxis

The bacterial chemotaxis, which is mediated by two-component systems, directs motile cells to favourable environments by controlling phosphorylation of histidine kinase CheA and its cognate response regulator CheY. Kinase activity is modulated by the chemoreceptors, which are in turn regulated by both the binding of chemoeffector and the level of methylation [39–41].

The expression of chemotaxis-related genes was strongly influenced by the inactivation of the RND pumps. The D4 and D4-D9 mutants shared 13 up-regulated chemotaxis-related genes with respect to *B. cenocepacia* J2315 (Table 5). These genes encoded MotA and MotB chemotaxis proteins (BCAL0126 and BCAL0127), the chemotaxis two-component sensor regulator (BCAL0128), and the sensor kinase CheA (BCAL0129). Moreover, the CheY2 (BCAL0135) and the CheZ (BCAL0136) encoding genes were up-regulated in both deleted strains, as well as other four genes coding for methyl-accepting chemotaxis proteins (BCAL0762, BCAM1424, BCAM1804, and BCAM2689), plus one methyl-transferase (BCAL0132), and one methyl-esterase (BCAL0134) (Table 5).

Furthermore, the D4 strain over-expressed other methyl-accepting chemotaxis proteins: (BCAL0131, BCAM1503, and BCAM2374), and BCAL0130 coding for the chemotaxis protein CheW. D4–D9 strain also over-expressed BCAL1452, coding for a methyl-accepting chemotaxis protein (Table 5). In contrast, in the D9 mutant no chemotaxis-related genes were over-expressed, while several of them were down-regulated (BCAL0129, BCAL0133, BCAL0134, BCAL0136) (Table 5; Figure S4).

Down-regulated genes

The genes that showed a decreased expression profile in D4 and D4–D9 mutants belonged to many different functional

Table 4. Motility and adherence related genes differentially expressed in *B. cenocepacia* D4, D9 and D4–D9 mutants respect to J2315.

Gene	Description	Change in gene expression (log_2 fold change)		
		D4 *vs* J2315	D9 *vs* J2315	D4–D9 *vs* J2315
BCAL0113	flagellar hook-associated protein	4.89	-	3.75
BCAL0114	flagellin	7.76	-	4.97
BCAL0124	flagellar regulon master regulator subunit FlhD	3.59	-	1.52
BCAL0125	flagellar regulon master regulator subunit FlhC	3.31	−1.16	2.03
BCAL0140	flagellar biosynthetic protein FlhB	3.78	−1.88	2.63
BCAL0142	flagellar biosynthesis protein FlhF	3.25	−0.82	2.28
BCAL0143	flagellar biosynthesis protein FlhG	4.53	-	1.85
BCAL0144	RNA polymerase sigma factor for flagellar	2.52	-	1.05
BCAL0520	putative flagellar hook-length control protein	2.98	−1.21	2.31
BCAL0521	flagellar fliJ protein	3.23	-	1.88
BCAL0522	flagellum-specific ATP synthase	3.55	−1.85	2.36
BCAL0523	flagellar assembly protein	3.73	-	2.16
BCAL0524	flagellar motor switch protein	2.03	-	-
BCAL0525	flagellar M-ring protein	2.16	-	-
BCAL0526	fliE flagellar hook-basal body complex protein FliE	2.19	-	-
BCAL0527	flagellar protein	3.243	-	2.89
BCAL0561	putative flagella synthesis protein	2.23	-	1.38
BCAL0562	putative negative regulator of flagellin	2.81	-	1.34
BCAL0564	putative flagellar basal-body Rod protein	3.44	-	-
BCAL0565	flagellar basal-body Rod protein	3.23	-	1.90
BCAL0566	putative basal-body Rod modification protein	4.88	−1.21	2.56
BCAL0567	putative flagellar hook protein	4.18	−1.31	2.36
BCAL0568	flagellar basal-body Rod protein	4.02	−1.34	2.43
BCAL0569	flagellar basal-body Rod protein	4.10	-	2.35
BCAL0570	flagellar L-ring protein precursor	3.14	−1.21	1.94
BCAL0571	flagellar P-ring protein precuror	2.85	−0.61	1.83
BCAL0576	putative flagellar hook-associated protein	4.41	-	-
BCAL0577	putative flagellar hook-associated protein	4.30	-	4.00
BCAL3501	flagellar biosynthetic protein	2.71	-	1.47
BCAL3503	flagellar biosynthetic protein	1.07	-	-
BCAL3505	probable flagellar motor switch protein	3.13	-	1.83
BCAL3506	flagellar motor switch protein FliM	2.58	-	-
BCAL3507	flagellar basal body-associated protein FliL	1.68	-	1.28
BCAM0777	putative flagellar motor proton channel	1.38	-	-
BCAM0778	putative flagellar motor protein	1.73	-	-
BCAM0987	putative flagellar basal body Rod protein	1.84	-	-
BCAM2758	cblS, two-component regulatory system. sensor kinase protein	1.33	-	-
BCAM2759	cblD, putative minor pilin and initiator	1.58	-	-

doi:10.1371/journal.pone.0018902.t004

classes. It was not possible to observe particularly representative classes because only a small number of the down-regulated genes were associated to each of many different metabolic processes. The under-expressed genes were mainly involved in basal metabolic processes of the cells, such as: macromolecule metabolic process, biopolymer modification, regulation of biosynthetic processes, regulation of cellular metabolic processes, cellular respiration and protein transport (Table S1, Figure S2 and S6). Strikingly, the down-regulated genes in mutant D9 belonged both to the motility/adherence and chemotaxis classes in contrast to the D4 and D4-D9 mutants which up-regulated this class of genes (Table S1, Figure S3). It is quite possible that the phenotype exhibited by the double mutant might be linked to D4 inactivation.

Table 5. Chemotaxis related genes differentially expressed in *B. cenocepacia* D4, D9 and D4-D9 mutants respect to J2315.

Gene	Description	Change in gene expression (log_2 fold change)		
		D4 vs J2315	D9 vs J2315	D4-D9 vs J2315
BCAL0126	chemotaxis protein MotA	3.43	-	2.27
BCAL0127	chemotaxis protein MotB	3.09	-	2.02
BCAL0128	chemotaxis two-component response regulator	3.32	-	2.44
BCAL0129	chemotaxis two-component sensor kinase CheA	3.52	-1.45	1.91
BCAL0130	chemotaxis protein CheW	2.99	-	-
BCAL0131	methyl-accepting chemotaxis protein I	1.48	-	-
BCAL0132	chemotaxis protein methyltransferase	3.48	-	1.49
BCAL0133	putative chemotaxis protein	3.33	-1.36	1.86
BCAL0134	chemotaxis protein-glutamate methylesterase	3.19	-0.83	1.73
BCAL0135	chemotaxis protein CheY2	2.55	-	1.34
BCAL0136	chemotaxis protein CheZ	2.48	-0.62	1.46
BCAL0762	putative methyl-accepting chemotaxis protein	1.96	-	1.58
BCAL1452	putative chemotaxis methyl-accepting membrane	-	-	0.69
BCAM1424	methyl-accepting chemotaxis protein	3.56	-	3.44
BCAM1503	putative methyl-accepting chemotaxis protein	1.87	-	-
BCAM1804	methyl-accepting chemotaxis protein	3.29	-	2.93
BCAM2374	putative methyl-accepting chemotaxis protein	1.45	-	-
BCAM2689	putative methyl-accepting chemotaxis protein	1.19	-	0.92

doi:10.1371/journal.pone.0018902.t005

Verification of microarray data by qRT-PCR

Evaluation of the fold change correlation between qRT-PCR experiments and microarray analysis was used to validate the over-expression and under-expression ratios observed in the microarray data (Table 6). 6 genes for each strain were chosen on the basis of their putative function, expression patterns and statistical reliability of the expression fold-change. The primers used are listed in Table 2.

For the D4 mutant strain the genes coding for the following proteins were chosen: the flagellin (BCAL0114), the chemotaxis protein CheY2 (BCAL0135), the putative DNA methyltransferase (BCAL0178), the putative flagellar hook-associated protein (BCAL0577), the putative RNA polymerase sigma factor (BCAL3152), and the putative HTH AraC family transcriptional regulator (BCAM2616). For the D9 mutant the following were selected: the flagellar biosynthetic protein FlhB (BCAL0140), the putative flagellar hook-length control protein (BCAL0520), the putative basal-body Rod modification protein (BCAL0566), two conserved hypothetical proteins (BCAM0726 and BCAM0727), and the putative response regulator BCAM1484 encoding genes. For the double mutant D4–D9 the following genes were chosen: BCAL0140, BCAL0520, BCAL0566, BCAL3152, the putative fimbrial usher protein encoding gene (BCAL1828), and the putative lipoprotein encoding gene BCAM0695. BCAM0166 (*ndh*, NADH dehydrogenase encoding gene) was used as internal reference gene. Over-expression and under-expression ratios were statistically consistent with the microarray findings and the overall trend of gene expression was similar for both microarray and qRT-PCR experiments for all the tested genes (Table 6), as shown by Pearson correlation (data not shown). A good linear correlation between both datasets was observed, with a coefficient of 0.85 ($p<0.01$) and a slope of 0.72.

Involvement of RND-4 and RND-9 efflux pumps in flagella-dependent phenotypes

Microarray analysis suggested that the RND-4 and RND-9 efflux pumps could play opposite roles in flagellum-dependent functions, like swimming and chemotaxis. To assess this hypothesis, these phenotypes were analyzed in the wild-type and in the RND-mutated strains, as described in Materials and Methods.

Data obtained revealed that single mutants D4 and D9 showed enhanced and reduced swimming motility with respect to the wild-type, respectively. Moreover, the D4–D9 mutant showed a swimming phenotype similar to that of the D4 mutant, suggesting that at least for this phenotype, mutation of RND-4 dominates over the mutation of RND-9 (Figure 2). These data were in full agreement with the microarray analysis, showing that flagellum-related genes are up-regulated in the D4 and D4–D9 mutants and down-regulated in the D9 mutant (Table 4).

Concerning chemotaxis, we have performed preliminary experiments using different attractant/repellents. The three mutants and the wild-type showed the same positive chemotactic phenotype versus casaminoacids and LB, and absence of chemotactic response using toluene, aztreonam and chloramphenicol as repellents (data not shown).

It is known that in many bacteria flagella could play a role also in adhesion and biofilm formation [42 and references therein]. Therefore, we performed a preliminary investigation about the ability of the four strains to produce biofilm by using two standard methods: adhesion to polyvinyl chloride microplates and Congo red binding. The two methods gave comparable results and, surprisingly, demonstrated that all the mutants showed enhanced biofilm formation, with respect to the wild-type (Figure 3).

Table 6. Fold change obtained in D4, D9 and D4–D9 microarray compared to the fold change obtained by qRT-PCR.

Gene	Description	Microarray log_2 fold change	qRT-PCR log_2 fold change
		D4	
BCAL0114	flagellin	7.76	7.47
BCAL0135	chemotaxis protein CheY2	2.55	0.62
BCAL0577	putative flagellar hook-associated protein	4.31	6.54
BCAL0178	putative DNA methyltransferase	−3.11	−10.45
BCAL3152	putative RNA polymerase sigma factor	−4.37	−2.23
BCAM2616	putative HTH AraC family transcriptional regulator	−1.97	−0.48
		D9	
BCAM0726	conserved hypothetical protein	1.71	2.38
BCAM0727	conserved hypothetical protein	1.24	2.93
BCAM1484	putative response regulator	0.58	0.19
BCAL0140	flagellar biosynthetic protein FlhB	−1.88	−1.14
BCAL0520	putative flagellar hook-length control protein	−1.21	−3.19
BCAL0566	putative basal-body Rod modification protein	−1.21	−2.86
		D4–D9	
BCAL0140	flagellar biosynthetic protein FlhB	2.63	2.28
BCAL0520	putative flagellar hook-length control protein	2.31	1.84
BCAL0566	putative basal-body Rod modification protein	2.56	3.03
BCAL1828	putative fimbrial usher protein	−5.25	−3.90
BCAL3152	putative RNA polymerase sigma factor	−3.96	−3.85
BCAM0695	putative lipoprotein	−6.75	−4.56

doi:10.1371/journal.pone.0018902.t006

Phenotype MicroArray analysis

To check the effect of the deletion of RND-4 and/or RND-9 operons on the phenotype of the strain *B. cenocepacia* J2315, a Phenotype MicroArray (PM) (Biolog) analysis was performed. Phenotype MicroArray [29,43] is a technology allowing to quantitatively measure thousands of cellular phenotypes all at once. Ten different panels (PM11-PM20) that enable chemical sensitivity tests for bacteria, were analyzed. A total of 240 chemicals at four different concentrations were tested out (a more detailed information about the PM panels is available at http://www.biolog.com). Data obtained are shown in Figure 4.

Principal component analysis (PCA) was applied to the PM data to study the differences between the phenotype profiles of the four strains in more detail (Figure 5). PCA separated the isolates into two groups by the first component (which accounted for 76.6% of phenotypic variation). One group housed wild-type and mutant D9, and the other included mutants D4 and D4–D9. The second component (which accounted for 12.7% of phenotypic variation) provided a fairly good separation of strains D4 and D4–D9, and did not allow the separation of wild-type and D9 mutant. These results suggested that D9 mutant has a phenotype very similar to that of the wild-type strain, while D4 is phenotypically different from the wild-type and similar to the D4–D9 mutant. The compounds under which the differences between the area of the kinetic curves of the wild-type and mutant strains were over 15000 Biolog units in at least one of the concentrations for each chemical assayed were selected and IC50 values are shown in Table S8. In agreement with the inactivation procedure used in this work, which makes use of a tetracycline resistance cassette, the three mutants exhibited a decreased sensitivity to minocycline, an antibiotic belonging to the tetracycline family. The mutants D4 and D4–D9 showed an increased sensitivity in respect to the wild-type to different types of compounds: antibiotics, DNA intercalators, drugs, fungicides, detergents, toxic anions, ionophores, uncouplers, oxidizing agents.

Discussion

In order to investigate the contribution of efflux pumps to intrinsic drug resistance of *B. cenocepacia* J2315, we recently deleted 3 operons encoding the putative RND transporters RND-1 (BCAS0591-BCAS0593), RND-3 (BCAL1674-BCAL1676), and RND-4 (BCAL2822-BCAL2820) [18]. We named the corresponding inactivated strains D1, D3, and D4. The *B. cenocepacia* D3 and D4 mutants demonstrated increased sensitivity to inhibitory compounds, suggesting an involvement of these proteins in the intrinsic drug resistance of *B. cenocepacia* J2315. In contrast, deletion of the RND-1 operon did not lead to detectable phenotype alterations under the conditions assayed [18]. In this work we continued in the same direction and analyzed the effect of the deletion of operon encoding RND-9 efflux pump (BCAM1945–1947 genes) in both the wild-type strain (thus obtaining D9 mutant), and in the D4 strain (thus obtaining the double D4–D9 mutant). Understanding the role of RND efflux transporters in *B. cenocepacia* is fundamental to highlight their involvement in drug resistance. Here, by integrating transcriptomics, phenomics, and a set of different phenotypic assays, we have expanded our previous work [18] and, in general, our knowledge on the role of this clinically important protein family. In particular, we have focused our attention on RND-4 and RND-9 efflux pump encoding operons, characterizing the deleted mutants D4, D9 and the double mutant D4–D9 by a combination

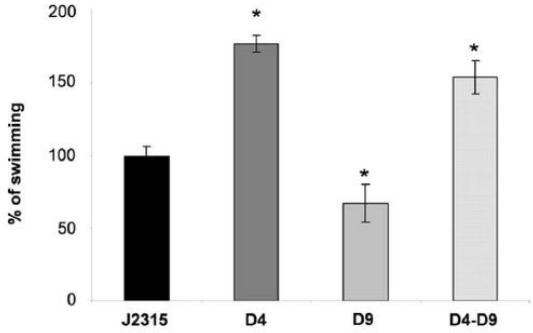

Figure 2. Effect of RND-4 and RND-9 mutations on swimming motility. The average diameter of swimming halos from three different experiments are plotted with standard deviations. Significantly differences with respect to J2315 are indicated by an * ($p<0.01$). Results are given in percentage, considering *B. cenocepacia* J2315 (wt) swimming halo as 100%. The panel below the graph shows one representative experiment. J2315, *B. cenocepacia* wild-type; D4, RND-4 mutant; D9, RND-9 mutant; D4-D9, RND4-RND9 mutant.
doi:10.1371/journal.pone.0018902.g002

of different experimental approaches. We used the Phenotype MicroArray (phenomic) procedure, a new technology that allows to quantitatively measure thousands of cellular phenotypes all at once, to check the ability of the wild-type and mutant strains to pump out different toxic metabolites. This phenomic analysis confirmed and strengthened previous data obtained by Buroni *et al.* [18] on mutant D4, showing that RND-4 is involved in the extrusion of a wide variety of compounds toxic for cell metabolism, in agreement with antimicrobial susceptibilities of the mutant as previously determined [18]. Similar results were obtained for the double mutant D4–D9.

Concerning mutant D9, the scenario is more intriguing; indeed, RND-9 seems to be only partially involved in drug efflux, showing MIC values only 2-fold lower than the wild-type strain for a few drugs, at least in our experimental conditions. These data are in full agreement with Phenotype Microarray analysis, which revealed that D9 mutant had a phenotype very similar to the wild-type strain. This opens the intriguing question of the role that this operon may play *in vivo*. However, since *B. cenocepacia* J2315 shows many genes involved in antibiotic resistance, many of which might have (partially) overlapping functions, it is quite possible that some of them might act in a synergistic fashion in determining the

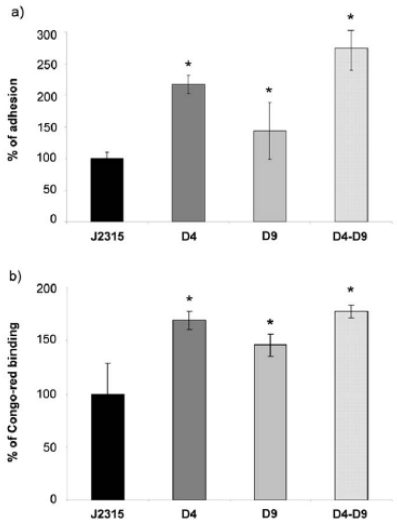

Figure 3. Effect of RND-4 and RND-9 mutations on biofilm formation. (A) Adhesion to polyvinyl chloride mitrotiter plates measured by crystal violet staining. (B) Congo red dye binding ability. In both cases, results are given as a percentage, considering *B. cenocepacia* J2315 (wild-type) as 100%. The mean of three different experiments with standard deviation is reported. Significantly differences with respect to J2315 are indicated by an * ($p<0.01$). J2315, *B. cenocepacia* wild-type; D4, RND-4 mutant; D9, RND-9 mutant; D4–D9, RND4-RND9 mutant.
doi:10.1371/journal.pone.0018902.g003

intrinsic resistance to one or more toxic compounds. So a two-fold decrease in MIC in the D9 deletion mutant is a proof that this pump may be involved in resistance to these antibiotics. Besides, as shown by Perrin *et al.* [17], BCAM1946 protein sequence (which appertains to RND-9 operon) belongs to the same phylogenetic cluster embedding BCAL2821 (which is part of RND-4), but to a different and distant branch, very close to the widely distributed RND-10 (BCAM2549-51); lastly, the phylogenetic distribution of RND-9 is very narrow, in that its orthologs were shown to be present only in a few Bcc species [17]. This might suggest that the absence of RND-9 function in D9 mutant could be replaced by other efflux systems, belonging to the same and/or to different phylogenetic clusters. An alternative, even though not mutually exclusive possibility, is that since the toxic compounds tested are not metabolic intermediates produced by *Burkholderia* cells, RND-9 is involved in the efflux of toxic (or even not-toxic) molecules produced by the microorganism under different physiological conditions.

The phenotypic similarity shared by mutants D4 and D4–D9 was confirmed also at the molecular level by the transcriptome analysis. Indeed, the microarray results showed that D4 and D4–D9 mutants have a similar expression profile, in particular motility and chemotaxis-related genes appear to be up-regulated in both strains. In contrast, the same genes are down-regulated or not differentially expressed in D9 mutant. Most differentially regulated genes of the single mutants were also differentially regulated in the double mutant, and for the most part in the same directionality. This illustrated how the double mutant displays a combined, additive expression profile of both single mutants and one would therefore expect to see an additive phenotype. The overall trend of gene expression was confirmed by qRT-PCR experiments by Pearson correlation, indicating that the microarray for *B. cenocepacia* is reliable to assess gene expression changes in this strain as has been shown in previous studies [21,44]. Moreover, data are consistent with the observations from the motility assays, in which the D4 and the double mutant show enhanced swimming motility with respect to the wild-type, in contrast with mutant D9 where this phenomenon is reduced. Moreover, D4 has 12 more up-regulated genes involved in motility than D4–D9, as reported in Table 4. This could be an explanation to the fact that this mutant is more motile than the double mutant D4–D9 (Fig. 2). In this view, it seems that D9 mutation is able to partially suppress the effects of the D4 mutation, at least for what concerns swimming.

Regarding chemotaxis, despite the differences observed in the microarray analysis, the three mutants showed the same chemotactic phenotype at least under our experimental conditions. It is possible that differences in chemotaxis might be appreciated by the use of specific attractant or repellent molecules. However, it is not trivial to identify such specific compounds and further studies should be performed in order to address this point.

These unexpected and interesting results strongly suggest that the biological role of the RND-4 and RND-9 efflux pumps might not be restricted to the sole transport of toxic (and/or not toxic) compounds, but also that their function might be related to motility and/or chemotaxis. To the best of our knowledge, this is the second time that the effect of RND efflux pumps mutation on motility-related phenotypes has been described. Indeed, the absence of RND components AcrB or TolC in *Salmonella enterica* caused widespread repression of chemotaxis and motility genes in these mutants, and for *acrB* mutant this was associated with decreased motility [45]. However, why the deletion of an efflux pump should have a fallout on bacterial motility and chemotaxis remains an open question. It is conceivable that the cytoplasmic accumulation of efflux pump-specific metabolites (different for each mutant) could act as signals triggering opposite behavioural response in the two mutants. For instance, we have recently shown that RND-4 contributes to the transport of *N*-acyl homoserine lactone (AHLs) as we found a reduced accumulation of AHLs quorum sensing (QS) signal molecules in the growth medium of D4 mutant [18]. Actually, the D4 and D4/D9 mutant produce about 30% less AHLs than the wild-type, while D9 produces almost the same level of acyl-HSL as the wild-type ([18] and Figure S7). In accordance with the low impact of D4 and D9 mutations on AHLs production, only few genes known to be AHL-regulated are also differentially regulated in our microarray analysis (Table S9). Among these, none can be directly related to chemotaxis or biofilm formation, and only BCAL0562 and BCAL3506 could be related to flagella. Overall, these observations suggest that it is unlikely that the phenotype of the D4, D9 and D4–D9 mutants is due to an unbalance in AHLs import/export rates. However, it cannot be ruled out that other molecules acting as metabolic signals could accumulate in the D4, D9 and D4–D9 mutants and account for the motility and biofilm phenotypes of these strains. Another possible explanation for the biological significance of the phenotype exhibited by D4 and D4–D9 strains might rely on the assumption that: i) the bacterial cell can "sense" the concentration of toxic compounds outside and/or inside the

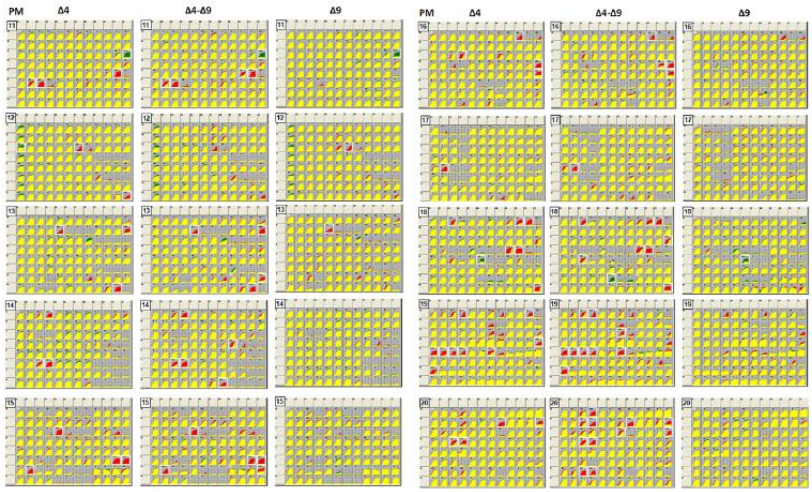

Figure 4. The Phenotype Microarray profile of *B. cenocepacia* J2315 and the RND mutants. Metabolic plates (from PM 11 to PM20) representing the growth of the three *B. cenocepacia* mutant strains D4, D9 and D4–D9 *versus* the wild-type strain J2315, in the presence of toxic compounds is shown.
doi:10.1371/journal.pone.0018902.g004

cell and that ii) the cell itself tries to respond to the increase of the concentration of toxic compound(s) by activating the efflux pump systems responsible for the extrusion of that compound(s). Accordingly, we can speculate that in the absence (such as in D4 and D4–D9 mutants) of these systems, the cell might somehow bypass this defect by increasing the ability to move in the environment in order to "escape" and to explore spaces and niches where the concentration of the toxic compounds is lower. In other words, the increased ability to move might represent a sort of "indirect protection" of the cell towards toxic compounds.

Since in many bacteria flagellum could play a role in biofilm formation, the different regulation of flagellum-related genes in D4 and D9 prompted us to speculate that these strains might also have opposite biofilm phenotypes. Therefore, we performed preliminary experiments to investigate the biofilm formation ability of the wild-type and of the three mutants. Results showed, surprisingly, that all the mutants had an enhancement of biofilm formation with respect to the wild-type. Therefore, differences in flagella expression in the D4 and D9 strains, with respect to the wild-type, play a minor role in biofilm formation, at least under our experimental conditions. The increased biofilm production of the RND-mutants was unexpected since we did not identify genes obviously involved in biofilm formation among the 33 having the same expression pattern in the three microarray experiments (Figure 1 and Table S1). Actually, biofilm formation is a complex pleiotropic phenotype, strongly dependent upon experimental conditions and growth media [46,47]. Therefore, it is not easy to correlate the microarray data derived from planktonic cultures with the increased biofilm production of the RND-mutants, with respect to the wild-type. However, 19 out of the 24 genes up-regulated in all the microarray experiments, are phage-related genes (located in the region spanning from ORFs BCAS0506 to BCAS0554; Table S1, Figure 1). Over-expression of phage-related genes in sessile cells compared with planktonic cells and/or increased expression in response to stress has been observed in several species [47 and references therein]. Bacterial stress response can increase the mobility of bacteriophages, and it has been proposed that prophage production may play a role in generating genetic diversity in the biofilm [47 and references therein]. It is tempting to speculate that cytoplasmic accumulation of toxic metabolites and/or metabolic signals due to the lack of RND-4 and/or RND-9 efflux pumps could produce a general stress response triggering the expression of genes involved in biofilm formation. This finding stimulates future studies on the role played by RND pumps in the efflux of endogenously produced molecules potentially involved in virulence and host colonization (*e.g.* biofilm matrix components, biologically active secondary metabolites, signal molecules), besides their role in drug resistance. The biofilm experiment also showed that D9 produces less biofilm than D4 and D4–D9. This result might be explained, at least in part, by the observation that, besides flagella genes, also cellulose biosynthetic genes (ORFs BCAL1391 and BCAL1395, Table S1) were up- and down-regulated in the D4 and D9 mutants, respectively, and the D9 showed down-regulation of fimbrial genes (ORFs BCAL0959 and BCAL2636, Table S1).

The different expression of genes involved in pathways strongly related to virulence is a first step towards a better understanding of *B. cenocepacia* pathogenesis. A relevant point is that inactivation of efflux pumps enhances biofilm formation and, sometimes, motility. If this is true also in the host, the use of efflux pump inhibitors

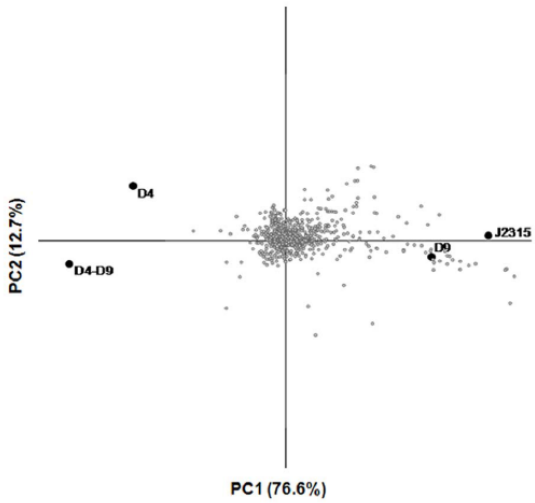

Figure 5. Principal component analysis of phenotype microarrays profiles of *B. cenocepacia* J2315 and D4, D9, D4–D9 mutants, obtained from an analysis of 960 chemical sensitivity tests (PM11-PM20). The figure shows the four strains (J2315, D4, D9, D4–D9) and the phenotypical tests plotted in an X-Y diagram corresponding to the first two components.
doi:10.1371/journal.pone.0018902.g005

could be, on one side positive for helping the antibiotic therapy, on the other side, it could promote biofilm formation and chronic infection. More detailed study on the effect of RND efflux pumps in virulence-related phenotype and chronic infection are strongly desirable.

In the future the construction of a multiple inactivated strain will be helpful both to understand if the lack of these proteins may affect pathways important for the life of the pathogen and, hopefully, to construct an attenuated strain, for the design of a suitable vaccine.

Supporting Information

Figure S1 Pie chart representing Gene Ontology (GO) terms distribution in *B. cenocepacia* D4 mutant up-regulated genes. Representation of the functional classes at the different nodes of one level in GO term association analysis.
(TIF)

Figure S2 Pie chart representing Gene Ontology (GO) terms distribution in *B. cenocepacia* D4 mutant down-regulated genes. Representation of functional classes at the different nodes of one level in GO term association analysis.
(TIF)

Figure S3 Pie chart representing Gene Ontology (GO) terms distribution in *B. cenocepacia* D9 mutant up-regulated genes. Representation of functional classes at the different nodes of one level in GO term association analysis.
(TIF)

Figure S4 Pie chart representing Gene Ontology (GO) terms distribution in *B. cenocepacia* D9 mutant down-regulated genes. Representation of functional classes at the different nodes of one level in GO term association analysis.
(TIF)

Figure S5 Pie chart representing Gene Ontology (GO) terms distribution in *B. cenocepacia* D4–D9 mutant up-regulated genes. Representation of functional classes at the different nodes of one level in GO term association analysis.
(TIF)

Figure S6 Pie chart representing Gene Ontology (GO) terms distribution in *B. cenocepacia* D4–D9 mutant down-regulated genes. Representation of functional classes at the different nodes of one level in GO term association analysis.
(TIF)

Figure S7 Evaluation of AHLs accumulation in the growth medium of *B. cenocepacia* J2315 and RND mutants. AHL measurement was carried out using *E. coli* (pSCR1) as described by Buroni *et al.* [18]. AHL was extracted from spent supernatants, AHL levels were measured with a volume of extract corresponding to 10^9 CFU. Values of AHL accumulated in the supernatant are in percentage in relation to the wild-type strain. The experiments were performed in triplicate giving comparable results. Significantly differences with respect to J2315 are indicated by an * ($p<0.05$). J2315, *B. cenocepacia* wild-type; D4, RND-4 mutant; D9, RND-9 mutant; D4–D9, RND4-RND9 mutant.
(TIFF)

Table S1 Complete list of genes up- or down-regulated in *B. cenocepacia* strains D4, D9, D4–D9 *versus* J2315 deriving from the microarray analysis.
(DOC)

Table S2 Gene Ontology (GO) terms functional enrichment analysis showing the over or under-representation of up-regulated genes of mutant D4 in comparison to *B. cenocepacia* J2315 whole genome functional annotation. Only GO terms over- or under- represented with an associated
p-value <0.05 are shown.
(DOC)

Table S3 Gene Ontology (GO) terms functional enrichment analysis showing the over or under-representation of down-regulated genes of mutant D4 in comparison to *B. cenocepacia* J2315 whole genome functional annotation.
(DOC)

Table S4 Gene Ontology (GO) terms functional enrichment analysis showing the over or under-representation of up-regulated genes of mutant D9 in comparison to *B. cenocepacia* J2315 whole genome functional annotation. Only GO terms over- or under- represented with an associated p-value <0.05 are shown.
(DOC)

Table S5 Gene Ontology (GO) terms functional enrichment analysis showing the over or under-representation of down-regulated genes of mutant D9 in comparison to *B. cenocepacia* J2315 whole genome functional annotation. Only GO terms over- or under- represented with an associated p-value <0.05 are shown.
(DOC)

Table S6 Gene Ontology (GO) terms functional enrichment analysis showing the over or under-representation of up-regulated genes of mutant D4-D9 in comparison to *B. cenocepacia* J2315 whole genome functional annotation. Only GO terms over- or under- represented with an associated p-value <0.05 are shown.
(DOC)

Table S7 Gene Ontology (GO) terms functional enrichment analysis showing the over or under-representation of down-regulated genes of mutant D4–D9 in comparison to *B. cenocepacia* J2315 whole genome functional annotation. Only GO terms over- or under- represented with an associated p-value <0.05 are shown.
(DOC)

Table S8 Schematic representation of data obtained from PM (from PM11 to PM20) analyses of *B. cenocepacia* strain J2315, D4, D9 and D4–D9. *IC50 was calculated on the basis of the kinetic curves obtained on the four different concentrations of each chemical compound and it was defined as the well or fraction of a well at which the area of kinetic curve is at half of its maximal value over the concentration series. **IC50 is reported only for compounds under which the difference between the areas of the kinetic curves of wild-type and mutant strain was over 15000 units in at least one of the concentrations tested.
(DOC)

Table S9 List of genes differentially regulated in *B. cenocepacia* strains D4, D9, D4–D9 *versus* J2315 known to be also controlled by AHL-based quorum sensing.
(DOC)

Acknowledgments

We thank Prof. P. Visca and Prof. E. De Rossi for helpful discussion.

Author Contributions

Conceived and designed the experiments: S. Buroni GR RF LL EM. Performed the experiments: S. Bazzini CU AS FL FD CV S. Buroni. Analyzed the data: S. Bazzini GE AS MF EP. Contributed reagents/materials/analysis tools: MRP LG LL RF EM GR. Wrote the paper: S. Buroni S. Bazzini LL RF AS EM GR.

References

1. LiPuma JJ (2010) The changing microbial epidemiology in cystic fibrosis. Clin Microbiol Rev 23: 299–323.
2. Foweraker J (2009) Recent advances in the microbiology of respiratory tract infection in cystic fibrosis. British Medical Bulletin 89: 93–110.
3. Mahenthiralingam E, Baldwin A, Dowson CG (2008) *Burkholderia cenocepacia* complex bacteria: opportunistic pathogens with important natural biology. J Appl Microbiol 104: 1539–1551.
4. Cunha LG Jr., Assis MC, Machado GB, Assef AP, Marques EA, et al. (2010) Potential mechanisms underlying the acute lung dysfunction and bacterial extrapulmonary dissemination during *Burkholderia cenocepacia* respiratory infection. Respir Res 18: 11–14.
5. Holden MT, Seth-Smith HM, Crossman LC, Sebaihia M, Bentley SD, et al. (2009) The genome of *Burkholderia cenocepacia* J2315, an epidemic pathogen of cystic fibrosis patients. J Bacteriol 191: 261–277.
6. Peeters E, Nelis HJ, Coenye T (2009) *In vitro* activity of ceftazidime, ciprofloxacin, meropenem, minocydin, tobramycin and co-trimoxazole on planktonic and sessile *Burkholderia cepacia* complex bacteria. J Antimicrob Chemother 64: 801–809.
7. Saiman L, Siegel J (2003) Cystic Fibrosis Foundation. Infection control recommendations for patients with cystic fibrosis: microbiology, important pathogens, and infection control practices to prevent patient-to-patient transmission. Infect Control Hosp Epidemiol 24: S6–52.
8. Nikaido H, Takatsuka Y (2009) Mechanisms of RND multidrug efflux pumps. Biochem Biophys Acta 179: 769–781.
9. Akama H, Kanemaki M, Yoshimura M, Tsukihara T, Kashiwagi T, et al. (2004) Crystal structure of the drug discharge outer membrane protein, OprM, of *Pseudomonas aeruginosa*: dual modes of membrane anchoring and occluded cavity end. J Biol Chem 279: 52816–52819.
10. Akama H, Matsuura T, Kashiwagi S, Yoneyama H, Narita S, et al. (2004) Crystal structure of the membrane fusion protein, MexA, of the multidrug transporter in *Pseudomonas aeruginosa*. J Biol Chem 279: 25939–25942.
11. Higgins MK, Bokma E, Koronakis E, Hughes C, Koronakis V (2004) Structure of the periplasmic component of a bacterial drug efflux pump. Proc Natl Acad Sci USA 101: 9994–9999.
12. Koronakis V, Sharff A, Koronakis E, Luisi B, Hughes C (2000) Crystal structure of the bacterial membrane protein TolC central to multidrug efflux and protein export. Nature 405: 914–919.
13. Murakami S, Nakashima R, Yamashita E, Yamaguchi A (2002) Crystal structure of bacterial multidrug efflux transporter AcrB. Nature 419: 587–593.
14. Piddock LJ (2006) Multidrug-resistance efflux pumps – not just for resistance. Nat Rev Microbiol 4: 629–636.
15. Ma Z, Jacobsen FE, Giedroc DP (2009) Coordination chemistry of bacterial metal transport and sensing. Chem Rev 109: 4644–4681.
16. Guglierame P, Pasca MR, De Rossi E, Buroni S, Arrigo P, et al. (2006) Efflux pump genes of the resistance-nodulation-division family in *Burkholderia cenocepacia* genome. BMC Microbiol 6: 66.
17. Perrin E, Fondi M, Papaleo MC, Maida I, Buroni S, et al. (2010) Exploring the HME and HAE1 efflux systems in the genus *Burkholderia*. BMC Evol Biol 10: 164.
18. Buroni S, Pasca MR, Flannagan RS, Bazzini S, Milano A, et al. (2009) Assessment of three Resistance-Nodulation-Cell Division drug efflux transporters of *Burkholderia cenocepacia* in intrinsic antibiotic resistance. BMC Microbiol 9: 200.
19. Flannagan RS, Linn T, Valvano MA (2008) A system for the construction of targeted unmarked gene deletions in the genus *Burkholderia*. Environ Microbiol 10: 1652–1660.
20. Coenye T, Van Acker H, Peeters E, Sass A, Buroni S, et al. (2011) Molecular mechanisms of chlorhexidine tolerance in *Burkholderia cenocepacia* biofilms. Antimicrob Agents Chemother. In press.
21. Drevinek P, Holden MT, Ge Z, Jones AM, Ketchell I, et al. (2008) Gene expression changes linked to antimicrobial resistance, oxidative stress, iron depletion and retained motility are observed when *Burkholderia cenocepacia* grows in cystic fibrosis sputum. BMC Infect Dis 8: 121.

22. Köhler T, van Delden C, Curty LK, Hamzehpour MM, Pechere JC (2001) Overexpression of the MexEF-OprN multidrug efflux system affects cell-to-cell signaling in *Pseudomonas aeruginosa*. J Bacteriol 183: 5213–5222.
23. Poole K (2001) Multidrug efflux pumps and antimicrobial resistance in *Pseudomonas aeruginosa* and related organisms. J Mol Microbiol Biotechnol 3: 255–264.
24. Sambrook J, Russell DW (2001) Molecular cloning: a laboratory manual. Cold Spring Harbor: Cold Spring Harbor Laboratory Press. 465 p.
25. Conesa A, Götz S, García-Gómez JM, Terol J, Talón M, et al. (2005) Blast2GO: a universal tool for annotation, visualization and analysis in functional genomics research. Bioinformatics 21: 3674–3676.
26. Rose H, Baldwin A, Dowson CG, Mahenthiralingam E (2009) Biocide susceptibility of the *Burkholderia cepacia* complex. J Antimicrob Chemother 63: 502–510.
27. Rampioni G, Schuster M, Greenberg EP, Zennaro E, Leoni L (2009) Contribution of the RsaL global regulator to *Pseudomonas aeruginosa* virulence and biofilm formation. FEMS Microbiol Lett 301: 210–217.
28. Leungsakul T, Keenan BG, Smets BF, Wood TK (2005) TNT and nitroaromatic compounds are chemoattractants for *Burkholderia cepacia* R34 and *Burkholderia* sp. strain DNT. Appl Microbiol Biotechnol 69: 321–325.
29. Bochner BR, Gadzinski P, Panomitros E (2001) Phenotype microarrays for high-throughput phenotypic testing and assay of gene function. Genome Res 11: 1246–1255.
30. Mahenthiralingam E, Urban TA, Goldberg JB (2005) The multifarious, multireplicon *Burkholderia cepacia* complex. Nat Rev Microbiol 3: 144–156.
31. Moens S, Vanderleyden J (1996) Functions of bacterial flagella. Crit Rev Microbiol 22: 67–100.
32. O'Toole GA, Kolter R (1998) Flagellar and twitching motility are necessary for *Pseudomonas aeruginosa* biofilm development. Mol Microbiol 30: 295–304.
33. Urban TA, Griffith A, Torok AM, Smolkin ME, Burns JL, et al. (2004) Contribution of *Burkholderia cenocepacia* flagella to infectivity and inflammation. Infect Immun 72: 5126–5134.
34. Feldman M, Bryan R, Rajan S, Scheffler L, Brunnert S, et al. (1998) Role of flagella in pathogenesis of *Pseudomonas aeruginosa* pulmonary infection. Infect Immun 66: 43–51.
35. Hayashi F, Smith KD, Ozinsky A, Hawn TR, Yi EC, et al. (2001) The innate immune response to bacterial flagellin is mediated by Toll-like receptor 5. Nature 410: 1099–1103.
36. Liaudet L, Szabo C, Evgenov OV, Murthy KG, Pacher P, et al. (2003) Flagellin from gram-negative bacteria is a potent mediator of acute pulmonary inflammation in sepsis. Shock 19: 131–137.
37. Hales BA, Morgan JA, Hart CA, Winstanley C (1998) Variation in flagellin genes and proteins of *Burkholderia cepacia*. J Bacteriol 180: 1110–1118.
38. Montie TC, Stover GB (1983) Isolation and characterization of flagellar preparations from *Pseudomonas* species. J Clin Microbiol 18: 452–456.
39. Hazelbauer GL, Falke JJ, Parkinson JS (2008) Bacterial chemoreceptors: high-performance signaling in networked arrays. Trends Biochem Sci 33: 9–19.
40. Hess JF, Oosawa K, Kaplan N, Simon MI (1988) Phosphorylation of three proteins in the signaling pathway of bacterial chemotaxis. Cell 53: 79–87.
41. Silversmith RE (2010) Auxiliary phosphatases in two-component signal transduction. Curr Opin Microbiol 13: 177–183.
42. Anderson JK, Smith TG, Hoover TR (2010) Sense and sensibility: flagellum-mediated gene regulation. Trends Microbiol 18: 30–37.
43. Bochner BR, Giovannetti L, Viti C (2008) Important discoveries from analysing bacterial phenotypes. Mol Microbiol 70: 274–280.
44. Peeters E, Sass A, Mahenthiralingam E, Nelis H, Coenye T (2010) Transcriptional response of *Burkholderia cenocepacia* J2315 sessile cells to treatments with high doses of hydrogen peroxide and sodium hypochlorite. BMC Genomics 11: 90.
45. Webber MA, Bailey AM, Blair JM, Morgan E, Stevens MP, et al. (2009) The global consequence of disruption of the AcrAB-TolC efflux pump in *Salmonella enterica* includes reduced expression of SPI-1 and other attributes required to infect the host. J Bacteriol 191: 4276–4285.
46. Coenye T (2010) Social interactions in the *Burkholderia cepacia* complex: biofilms and quorum sensing. Fut Microbiol 5: 1087–1099.
47. Coenye T (2010) Response of sessile cells to stress: from changes in gene expression to phenotypic adaptation. FEMS Immunol Med Microbiol 59: 259–252.